

# **Journal of Mechanics and Structure**

**Volume No. 12**

**Issue No. 1**

**January - April 2024**



**ENRICHED PUBLICATIONS PVT. LTD**

**S-9, II<sup>nd</sup> FLOOR, MLU POCKET,  
MANISH ABHINAV PLAZA-II, ABOVE FEDERAL BANK,  
PLOT NO-5, SECTOR-5, DWARKA, NEW DELHI, INDIA-110075,  
PHONE: - + (91)-(11)-47026006**

# Journal of Mechanics and Structure

## **Aims and Scope**

Journal of Mechanics Structural is a journal which offers prompt publication of structural design; this journal publishes peer-reviewed technical papers on state-of-the-art topics and future developments of the profession. Engineers, consultants, and professors detail the physical properties of engineering materials (such as steel, concrete, and wood), develop methods of analysis, and examine the relative merits of various types of structures and methods of fabrication. Subjects include the design, erection, and safety of structures ranging from bridge to transmission towers and tall buildings; technical information on outstanding, innovative, and unique projects; and the impact of natural disasters and recommendations for damage mitigation.

# Journal of Mechanics and Structure

**Managing Editor**  
**Mr. Amit Prasad**

<p><b>Dr. Pabitra Rajbongshi</b> Asso. Prof. Civil Engineering Dept. NIT Silchar E-mail: prajbongshi@yahoo.com</p>	<p><b>Mohd. Masroor Alam</b> Asso. Prof. Engineering Geology Dept. of Civil Engineering Aligarh Muslim University masroor8497@rediffmail.com</p>
--	--

# Journal of Mechanics and Structure

(Volume No. 12, Issue No. 1, January - August 2024)

## Contents

Sr. No.	Title / Authors Name	Pg. No.
1	Experimental Investigation of the Performance Characteristics of a Spark Ignition Engine by Varying the Compression Ratio - <i>P. Goyal, S.K. Sharma, Amit Pal</i>	01 - 07
2	A Case Study of Vapour Absorption System based on Waste Heat at AIIMS, New Delhi - <i>Md. Nawaz Khan, M.N.Karimi, Pardeep Kumar, Md. Mamoon Khan, Subhash Chand</i>	08 - 19
3	Optimization of Surface Grinding Parameters for Flat Surface of AISI D3 using RSM - <i>Umesh Kumar Vates, Gyanendra Kumar Singh, Vivek Kumar, Shubham Sharma</i>	20 - 32
4	A Review on Room Temperature Magnetic Refrigeration for Domestic Applications - <i>Mohammad Talha Javeda, Naved Azumb</i>	33 - 56
5	Development of Risk Based Maintenance Strategy For Gas Turbine Power System - <i>Asis Sarkar, D.K. Behera</i>	57 - 72

# Experimental Investigation of The Performance Characteristics of A Spark Ignition Engine By Varying The Compression Ratio

P. Goyal<sup>1</sup>, S.K. Sharma<sup>2‡</sup>, Amit Pal<sup>3</sup>

<sup>1</sup>Amity Institute of Aerospace Engineering, Amity University Uttar Pradesh, India

[priyankagoel03@gmail.com](mailto:priyankagoel03@gmail.com)

<sup>2</sup>Quality Assurance Enhancement Department, Amity University Uttar Pradesh, India

[Sks15nov@gmail.com](mailto:Sks15nov@gmail.com)

<sup>3</sup>Department of Mechanical Engineering, Delhi Technological University, Delhi, India

[amitpal@dce.ac.in](mailto:amitpal@dce.ac.in)

<sup>‡</sup>Corresponding Author; Tel: +91 8800987446

## **ABSTRACT**

*The Spark Ignition Engine has been extensively used in various sectors viz. Automobile industries, etc. In today's scenario, there is a huge need to improve the performance characteristics of the spark ignition engine. Compression ratio is a major factor which plays an important role in the spark ignition engine and it has a greater influence also on the performance characteristics of an internal combustion engine. The present research paper shows an experimental investigation of the effect of compression ratio on the performance characteristics which are brake power, brake thermal efficiency, brake mean effective pressure and specific fuel consumption of the spark ignition engine. Different compression ratios with different engine speeds were used in the present study. This work shows that there is a remarkable decrement in the specific fuel consumption with an increased compression ratio and improved brake power, brake thermal efficiency and brake mean effective pressure.*

**Keywords** - Spark Ignition engine; compression ratio; engine speed; brake power; specific fuel consumption.

## **1. INTRODUCTION**

Improving efficiency of an Internal Combustion Engine is a major concern in today's fast growing automobiles sector. Higher compression ratio is one of the very useful and important aspects to improve the fuel consumption and power output in gasoline engines as combustion efficiency increases with the compressed air and fuel mixture [1]. Most of the energy produced by these engines lost in the form of heat. There is a number of other losses also associated with the engine like friction losses and losses of the exhaust and some other parameters which also affects the thermal efficiency of the engine [2,3,4].

Compression Ratio (CR) is the ratio of the total volume of the combustion chamber when the piston is at bottom dead centre to the total volume of the combustion chamber when the piston is at top dead centre [5]. Lots of research has been devoted to the effect of the higher compression ratio of a spark ignition engine.

The main challenge is that the conventional gasoline engines operate at an optimal compression ratio, which is set low enough to prevent premature ignition of the fuel, or knock, at high power levels under fast acceleration, high speeds or heavy loads. But, most of the time, gasoline engines operate at relatively low power levels under slow acceleration, lower speed, or light loads.

## **VCR Engine**

A variable compression ratio (VCR) engine is able to operate at different compression ratios, depending on the particular vehicle performance needs. The VCR engine is optimized for the full range of driving conditions, such as, acceleration, speed and load. At low power levels, the VCR engine operates at high compression to capture the benefits of fuel efficiency, while at high power levels, it operates at low compression levels to prevent knock. To further improve the fuel economy, the VCR engine is small, with about one-third the displacement volume of a conventional gasoline engine [6].

## **VCR Concepts**

Conventionally, every mechanical element in the power conversion system has been considered a way to achieve a variable compression ratio. Many designs presented solved by various researchers which modifies the compression ratio by the following methods [7]:

- ❑ Moving the cylinder head;
- ❑ Variation of combustion chamber volume;
- ❑ Variation of piston deck height;
- ❑ Modification of connecting rod geometry;
- ❑ Moving the crankshaft axis;

In many cases, the deviation from conventional production engine structure or layout represents a significant commercial barrier to wide spread adoption of the technology.

## **Applications of VCR Engines**

The concept of a variable compression ratio promises improved engine performance, efficiency and reduced emissions also [6,7].

- ❑ Higher compression ratio gives faster laminar flame speed. Therefore, the ignition delay period is shorter. As a result, at low loads, the greater the compression ratio, the shorter is the combustion time. Time loss is subsequently reduced. Therefore, it seems reasonable that fuel consumption rate is lower with high compression ratios at part load.

- ❑ The VCR can make a significant contribution to thermodynamic efficiency. A VCR engine can continuously vary the compression ratio by changing the combustion chamber volume. In a VCR engine, thermodynamic benefits appear throughout the engine map.
- ❑ The optimum compression ratio is determined as a function of one or more vehicle operating parameters such as inlet air temperature, engine coolant temperature, exhaust gas temperature, engine knock, fuel type, octane rating of fuel etc. In a VCR engine, the operating temperature is more or less maintained at optimum, where combustion efficiency is high.

This paper specifically discusses the effect of a variable compression ratio on the performance characteristics of a spark ignition engine. One researcher conducted a research on the effect of the higher compression ratio in two-stroke engines and showed that the actual fuel consumption was improved by 1-3% for each unit increment in the compression ratio [8]. Power output also improves, but the maximum compression ratio is limited because of the knock and the thermal loads. It was also noticed that the rate of improvement was lesser compared with the theoretical values. But these redundancies were due to the mechanical, cooling losses and mainly due to the thermal losses which were explained above. Similarly, experiments performed on four-stroke a petrol engine which also shows the remarkable increment in the mechanical efficiency and thermal efficiency of a spark-ignition engine [9,10].

## 2. EXPERIMENTAL SET-UP

The schematic diagram of the experimental setup is shown in Fig. 1. The performance characteristics like brake power, brake thermal efficiency, brake mean effective pressure and specific fuel consumption have been measured with varying compression ratio of 5 to 9 at different engine speed of 1300 to 1600 RPM with the each increment of 100rpm of a spark ignition engine. The specifications of the test engine are shown in Table 1.

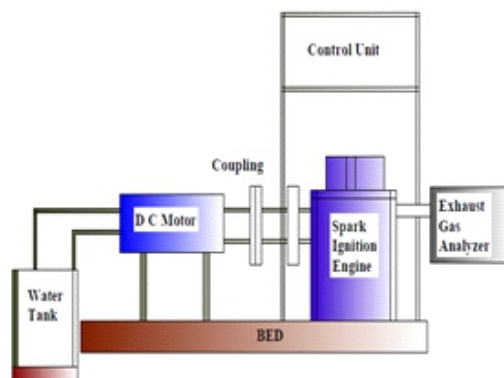


**Fig. 1.** A systematic layout of test setup

**Table 1.** Specification of the Experimental Set up

Item	Specification
Engine Type	Single Cylinder 4 Stroke Engine
Fuel	Gasoline
Cooling system	Water cooled
Stroke (mm)	110
Bore (mm)	80
Compression ratio	9.2:1
Spark variation range	0-70 btdc
Type of Injection	Direct Injection
Injection Pressure (bar)	200
Load Indicator	Digital, range 0-50 kg, supply 230V, AC

### 3. RESULTS AND DISCUSSION

The following graphs were obtained by the experimental analysis for brake power, brake thermal efficiency, brake mean effective pressure and specific fuel consumption by varying the compression ratio at different engine speed.

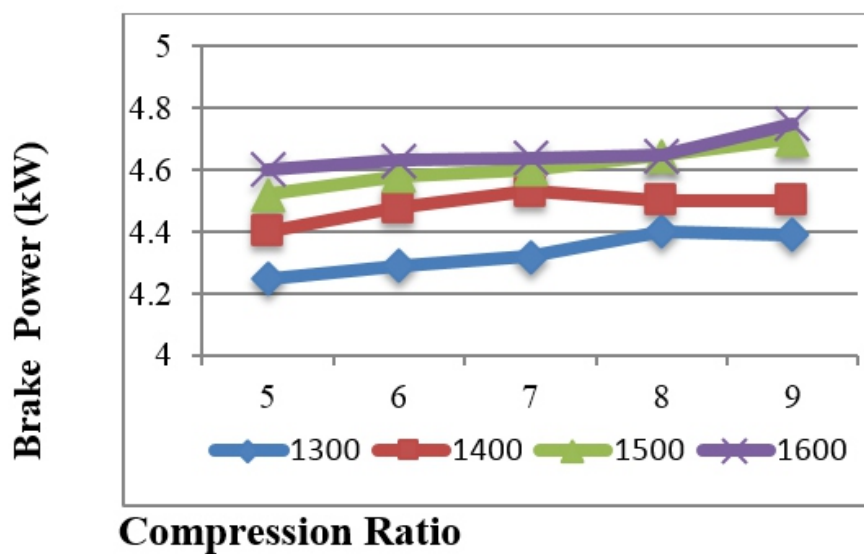


**Fig. 2.** Variation of brake power with compression ratio at different engine speed.



**Brake Power (kW):** In the comparative analysis of brake power with compression ratio of different engine speed as shown in Fig 2. It is observed that brake power increases with the compression ratio. This is mainly due to the increase in brake torque at high compression ratios. Engine torque is directly related to brake power which is a theoretical fact. Therefore, as the engine gives more push on the piston, and then more torque is generated.

**Brake Mean Effective Pressure (bar):** In the comparative analysis of brake power with compression ratio of different engine speed as shown in Fig. 3. It is observed that brake mean effective pressure increases with the compression ratio. But the lowest increase in the pressure occurs at the 1400 RPM and it is more or less constant from the compression ratio 6 to 9 at engine speed of 1400 RPM. The highest increment in the pressure occurs at a compression ratio of 9.

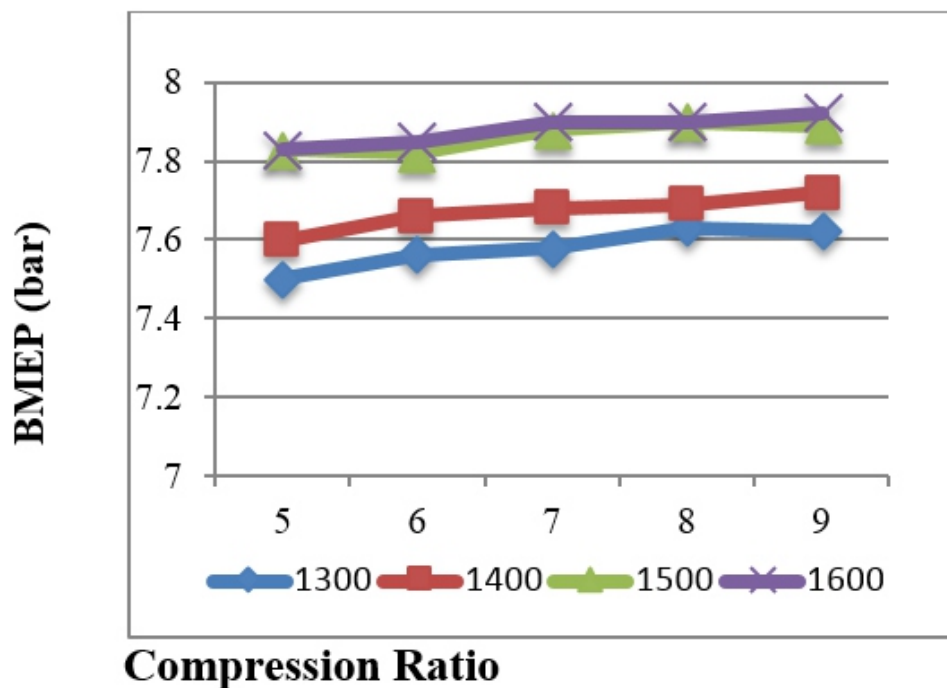


**Fig. 3.** Variation of brake mean effective pressure with compression ratio at different engine speed.

**Brake Thermal Efficiency (%):** In the comparative analysis of brake thermal efficiency with compression ratio of different engine speed as shown in Fig. 4. The graph clearly shows that the brake thermal efficiency is maximum at a higher compression ratio. Better mixing and evaporation of the fuel occurs with the greater compression of the available fuel and air. As the compression ratio increases, combustion efficiency also increases, which results in the remarkable increment in the energy also.

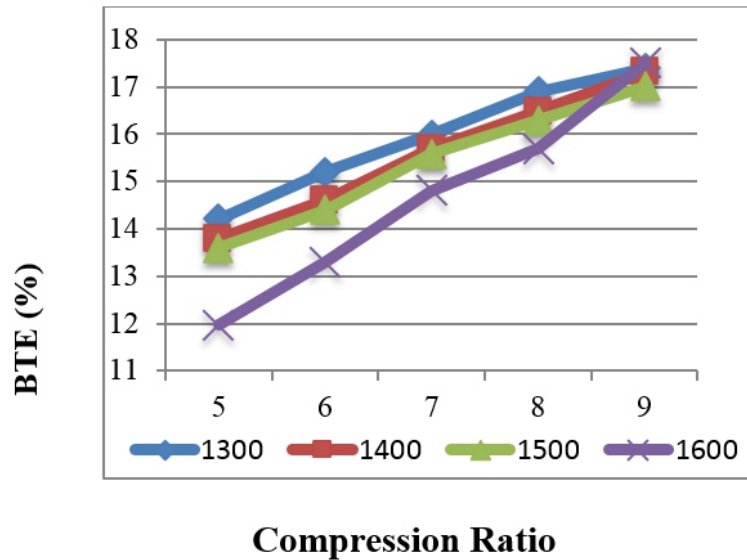


**Fig. 4.** Variation of brake thermal efficiency with compression ratio at different engine speed.

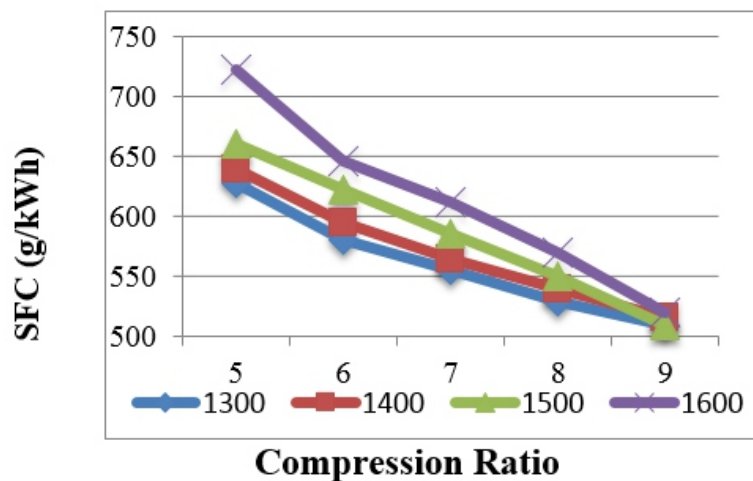


**Fig. 5.** Variation of specific fuel consumption with compression ratio at different engine speed.

**Specific Fuel Consumption (g/kWh):** In the comparative analysis of specific fuel consumption with compression ratio at different engine speed as shown in Fig. 5. It is shown that the less fuel is required at higher compression ratios as the fuel mixture is effectively compressed which causes the higher thermal efficiency. Result in the reduced fuel consumption at higher compression ratio.

#### 4. CONCLUSION

As from the above result, we can conclude that the increase in the compression ratio improves the overall efficiency of an engine. It also improves the fuel consumption with the each unit of increment in the compression ratio. Brake thermal efficiency shows the increment of 3-6% for each unit increase of

compression ratio. Brake power, brake mean effective pressure also shows a remarkable increment for the higher compression ratio. There is a considerably higher difference in the theoretical and experimental results which is primarily because of the thermal, mechanical and frictional losses. To further enhance the efficiency of an engine alternative fuels are the best option with the higher compression ratio and can be incorporated with the number of different design parameters.

## REFERENCES

- Andreas, B., “Torque Modeling and Control of a Variable Compression Engine”, Dept. of Electrical Engineering at Linkopings University, Sweden. 2003. (Master's Thesis)
- [1] David Gerard, Magali Besson, Marc Thomine “HCCI combustion in a diesel VCR engine” SAE 2008-01-1187 April 14<sup>th</sup> 2008. (Article)
- [2] F.H Palmer, “Vehicle performances of gasoline containing oxygenates”, International conference on petroleum based fuels and automotive applications, London, UK; pp. 33–46, 1986. (Conference Paper)
- [3] Maurillio, Marco Lucio, Sergio Gradella Villalva “Variable compression ratio engines” SAE 2009-36-0245 October 10<sup>th</sup> 2009. (Article)
- [4] Heywood J. B., *Internal combustion Engines Fundamentals*. McGraw Hill Book Company, pp.450-458, 1988. (Book)
- [5] R G Sykes, Tickford, *Engines Expo 2000 paper*, “Methods to reduce the fuel consumption of gasoline engines”. (Conference)
- [6] J R Clarke, R J Tabaczynski, US Patent 6135086, 2000-10-24, “Internal combustion engine with adjustable compression ratio and knock control”. (Patent)
- [7] Yuh, M. and Tohru, G., 2010, “The Effect of Higher Compression Ratio in Two-Stroke Engines”, Yamaha Motor Co, Ltd. pp 355-362. (Article)
- [8] Rychter T.J., Teodorczyk A., Stone C.R., Leonard H.J., Ladommatos N. and Charlton S.J. “A theoretical study of a variable compression ratio turbocharged diesel engine”. Vol.206, Part A: *Journal of Power and Energy*, 1992, pp.227-238. (Article)
- [9] C.L. Song, W.M. Zhang, Y.Q. Pei, G.L. Fan, G.P. Xu, “Comparative effect of MTBE and ethanol addition into gasoline on exhaust emission”, *Atmospheric environment*, pp. 403-410, 2006. (Article)

# A Case Study of Vapour Absorption System based on Waste Heat at AIIMS, New Delhi

<sup>1</sup>Md. Nawaz Khan, <sup>2</sup>M.N.Karimi, <sup>3</sup>Pardeep Kumar, <sup>4</sup>Md. Mamoon Khan,  
<sup>5</sup>Subhash Chand

<sup>1</sup>Department of Mechanical Engineering, Alfalah University, Faridabad, Haryana, India

<sup>2</sup>Department of Mechanical Engineering, Jamia Millia Islamia, New Delhi, INDIA

<sup>3</sup>A.E (Electrical), AIIMS, New Delhi, INDIA

<sup>4</sup>Department of Mechanical Engineering, Rohilkhand University, Bareilly, U.P, INDIA

<sup>5</sup>J.E (R.A.C), AIIMS, New Delhi, INDIA

## **ABSTRACT**

*In this paper performance assessment of a vapor absorption system based on waste heat plant and its comparison to the conventional chiller plant in operation for the duration of 2015 at Jai Prakash Narayan Apex Trauma Centre, AIIMS, New Delhi. The tri-gen plant includes DG set, VAM of cooling capacity 105TR and centrifugal chiller of 250Tr. The study reveals that the trigen plant is no more economical compare to conventional electrical chiller because of PNG price hike. If the trauma centre get the PNG at subsidized rate, the PNG plant will again run in profit. An idea is also suggested to run the VAM at the time of base load demand by providing the additional heat by direct burning of PNG and regulating the flow of PNG by electronic controlled flow valve.*

**Keywords:** VAM, PNG, Chiller, Trigenation

## **1. INTRODUCTION**

Utilization of energy in buildings in the search of thermal comfort has become an important issue on a global scale. Mainly conventional compression system has been used for air conditioning of the building and now there is also an option of Vapor Absorption system based on waste heat from various sources. A Vapor Absorption Machine based on waste heat source of Diesel Generator set has been installed by All India Institute of Medical Sciences at their Jai Prakash Narayan Apex Trauma Centre and a case study of that system is done in this paper.



**Fig. 1.** Jai Prakash Narayan Apex Trauma Centre

## **2. LITERATURE REVIEW**

S. Manoj Prabhakar et al. (2014) has reduced the fuel consumption by using exhaust gas waste heat. His work presents an experimental study refrigeration system, using vapour absorption system. This system uses the exhaust waste heat of an internal combustion engine as energy source. The system was found to be applicable and ready to produce the required conditioning effect without any additional load to the engine. Parfait Tatsidjodoung et al. (2013) has reviewed the thermal energy storage technologies suitable for building applications with a particular interest in heat storage materials. He provides an insight into recent developments on materials, their classification, their limitations and possible improvements for their use in buildings. R.B. Lokapure et al. (2012) in his research the main stress is given on energy conservation by using technique of utilizing waste heat from Air-conditioning system and increasing COP. The target of improving COP was up to 20 %, but in this case we achieved our goal by recovering energy and improving COP up to 13%.

K.Balaji et al. (2012) in his paper illustrates the thermal and fiscal advantages of using single effect lithium bromide water absorption by means of waste heat. The objective of his work is to hypothetical design of lithium bromide water absorption Refrigeration system using waste heat from sugar industry steam turbine exhaust. The Overall heat transfer coefficient, effectiveness and COP of the heat exchanger are measured .S. Mekhilef et al. (2011) reviewed on solar energy and he found that solar thermal is getting remarkable popularity in industrial applications and it's also an alternative to generate electricity, process chemicals or even space heating. It can be used in food, non-metallic, textile, building, chemical or even business related industries. O. Marc et al. (2010) in his paper presents an experimental study of a solar cooling absorption system implemented in Reunion Island, located in the southern hemisphere near the Capricorn Tropic. The particularity of this project is to achieve an effective cooling of classrooms, by a solar cooling system without any backup systems (hot or cold).

R.Z. Wang et al. (2009) discussed the various typical systems with small scale for potential residential applications, in which the working principals, system suitability for solar cooling, performance, maintenance and economic viability. With such analyses and the available real operation systems, the detailed options and guidelines of solar cooling for residential applications are shown. Tiago Mateusa et al. (2009) in his study aims to evaluate the potential of integrated solar absorption cooling and heating systems for building applications. The TRNSYS software tool was used as a basis for assessment. Different building types were considered: residential, office and hotel. The TRNSYS models are able to run for a whole year (365 days), according to control rules (self-deciding whether to operate in heating or cooling modes), and with the possibility of combining cooling, heating and DHW applications. Three different locations and climates were considered: Berlin (Germany), Lisbon (Portugal), and Rome (Italy). Both energy and economic results are presented for all cases. Balarasa et al. (2009) describes the main results of the EU project SACE (Solar Air Conditioning in Europe), aimed to assess the state-of-the-art, future needs and overall prospects of solar cooling in Europe. A group of researchers from five countries has surveyed and analyzed over 50 solar-powered cooling projects in different climatic zones. The paper presents a short overview on the state-of-the-art and potential of solar-assisted cooling and air conditioning technologies. M. Balghouthi et al. (2008) in his paper, he present a research project aiming at assessing the feasibility of solar-powered absorption cooling technology under Tunisian conditions. Simulations using the EES programs with a meteorological year data file containing the weather parameters of Tunis, the capital of Tunisia.

Ahmed Hamza et al. (2008) do the performance assessment of an integrated cooling plant having both free cooling system and solar powered single-effect lithium bromide–water absorption chiller in operation since August 2002 in Oberhausen, Germany. The monthly average collectors' field efficiency value varies from 34.1% up 41.8% and the five-year average value amounts about 28.3%. Clito F et al. (2006) in his work done a review of cooling systems in buildings discussing both classical and more advanced technology emerging from recent research, with a respect to their general operating principles and their applications. In his paper a classification of cooling systems is presented according to the final energy used to operate them. Y.L. Liu et al. (2005) introduced newly developed adsorption water chiller and tested. In the new adsorption refrigeration system, there are no refrigerant valves. Silica-gel–water is used as working pair and mass recovery-like process is adopted in order to use low temperature heat source ranging from 70 to 85°C effectively and the experimental data demonstrate that the chiller performance has been greatly improved, with a heat source temperature of 80°C, a COP over 0.5 and cooling capacity of 9 kW has been achieved at evaporating temperature of 13°C. A. Syed et al. (2005) reports novel experimental results derived through field testing of a part load solar energized cooling system for typical Spanish houses in Madrid during the summer period of 2003. The results



clearly demonstrate that the technology works best in dry and hot climatic conditions where large daily variations in relative humidity and dry bulb temperature prevail. This case study provides benchmark data for the assessment of other similar prototypes and for the validation of mathematical models. R.Z. Wang et al. (2005) presented the prototypes which were designed to use waste heat or solar energy as the main heat sources. The waste heat could be from diesel engines or from power plants, in combined cooling, heating and power systems (CCHP). The utilization of such chillers in CCHP systems, hospitals, buildings and grain depots are discussed. Despite their advantage, solid sorption systems still present some drawbacks such as low specific cooling power and COP. B.B. Sahaa et al. (2003) in his paper evaluate the performance of dual-mode silica gel–water adsorption chiller. This adsorption chiller utilizes effectively low temperature solar or waste heat sources of temperature between 40 and 95 °C. The first operation mode will be to work as a highly efficient conventional chiller where the driving source temperature is between 60 and 95 °C. The drawback of this operational mode is its poor efficiency in terms of cooling capacity and COP. B.B. Saha et al. (2003) in his paper, a three-bed non-regenerative silica gel–water adsorption chiller design is outlined along with the performance evaluation of the innovative chiller. The three-bed chiller will be able to work as high efficient single-stage adsorption chiller where driving source temperature is between 60 and 95°C along with a coolant at 30°C. This facilitates the maximum utilization of the waste stream. The delivered chilled water temperature is about 6°C with this operation condition. Simulation results also show that from the two to three beds, waste heat recovery efficiency is boosted by about 35%. Nelson Fumo et al. (2002) presents the results from a study of the performance of a packed tower absorber and regenerator for an aqueous lithium chloride desiccant dehumidification system. The rates of dehumidification and regeneration, as well as the effectiveness of the dehumidification and regeneration processes were assessed under the effects of variables such as air and desiccant flow rates, air temperature and humidity, and desiccant temperature and concentration. A Elsafty et al. (2002) presents an analysis of the general cost associated with single- and double-effect vapour absorption and vapour compression air-conditioning systems. The cost analysis covers the initial costs and the operating costs of each of the three systems. The vapour absorption system considered in this paper is based on water as the refrigerant and lithium bromide solution as the absorbent. The analysis is undertaken to help select an air-conditioning system that fulfils a 250 TR cooling load of a five-floor student hospital in Alexandria, Egypt. The typical meteorological year database for Alexandria was used to estimate the cooling load for the building. B.B. Sahaa et al. (2001) proposed two-stage non-regenerative adsorption chiller design and experimental prototype is proposed. In his study silica gel–water is taken as the adsorbent refrigerant pair. To exploit waste heat of temperatures below 70°C, staged regeneration is necessary. The two-stage cycle can be operated effectively with 55°C waste heat in combination with a 30°C coolant temperature. Z.F. Li et al. (2000) in his work various solar powered heating systems tested

extensively, but solar powered air-conditioners have received little more than short-term demonstration attention. This paper reviews past efforts in the field of solar powered air-conditioning systems with the absorption pair of lithium bromide and water.

### 3. SYSTEM DESCRIPTION

The vapour absorption refrigeration is heat operated system. In the absorption system the compressor of the vapour compression system is replaced by the combination of “absorber” and “generator”. A solution known as the absorbent, which has an affinity for the refrigerant used, is circulated between the absorber and the generator by a pump (solution pump). The absorbent in the absorber draws the refrigerant vapour formed in the evaporator thus maintaining a low pressure in the evaporator to enable the refrigerant to evaporate at low temperature. In the generator the absorbent is heated.

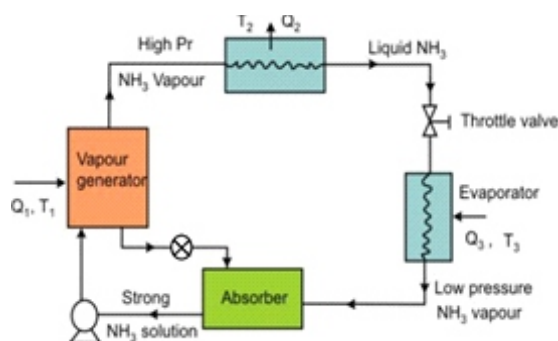


**Fig. 2.** Vapour Absorption System

There by releasing the refrigerant vapour (absorbed in the absorber) as high pressure vapour, to be condensed in the condenser. Thus the suction function is performed by absorbent in the absorber and the generator performs the function of the compression and discharge. The absorbent solution carries the refrigerant vapour from the low side (evaporator–absorber) to the high side (generator–condenser). The liquefied refrigerant flows from the condenser to the evaporator due to the pressure difference between the two vessels; thus establishing circulation of the refrigerant through the system.

### 4. METHODOLOGY

The analysis done is based on data available for running system of JPNATC, AIIMS. The system consisting of PNG operated Diesel Generating (DG) Set, Chiller, Vapour Absorption Machine (VAM) etc.

A piped natural gas is provided by the Indraprastha Gas limited to the trauma centre of AIIMS. PNG is fed to the DG Set which produces electricity of 347 kW which is used to run the chiller plant of 150Tr



and remaining is used to run the utilities. The exhaust from the DG set as a low grade thermal energy is supplied to the Vapour Absorption Machine which produces cooling effect and supplied the chilled water to the common header. In order to meet the cooling load of trauma centre additional to the Trigen Plant, two chiller plant of 200Tr capacity is also used which is run by electricity provided by NDMC.

### Specifications of Trigen Plant

- I) Makers of DG Set: Schmitt Enertec
- ii) Capacity of DG Set: 347 kWe
- iii) Exhaust Gas Temperature: 400 °C
- iv) Makers of Centrifugal Chiller:
- v) Centrifugal Chiller Plant: 250 Tr
- vi) Makers of VAM: Thermax
- vii) Capacity of VAM: 105 Tr
- viii) Low Temp. Heat Source: Exhaust Gas
- ix) Inlet Pressure: 0.07bar
- x) Power Supply: 415V

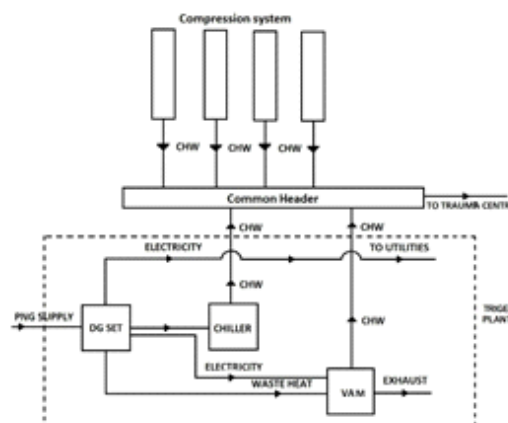


**Fig. 3.** Block Diagram of Trigen Plant



**Fig. 4.** DG Set, 347 kWe, Schmitt Enertec make



**Fig. 5.** VAM, 105Tr, Thermax make



**Fig. 6.** Centrifugal Compressor, 250Tr, York Make

**Table 1.** Monthly electricity consumption by electrical chiller

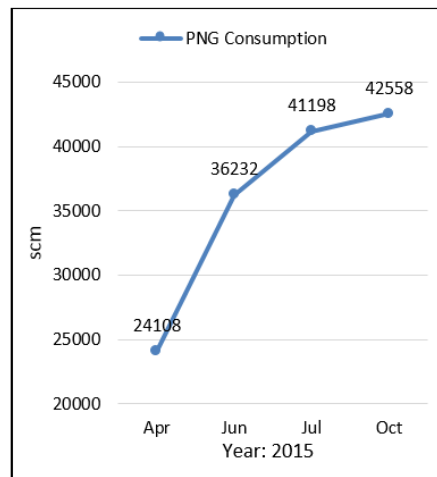
Months	TRH	kWh
Jan	20,041	14,233
Feb	33,250	23,310
Mar	112,151	74,406
Apr	124,782	88,472
May	170,384	119,206
Jun	202,207	140,717
July	229,993	161,675
Aug	222,877	155,745
Sep	196,609	137,923
Oct	167,084	117,075
Nov	54,643	38,198
Dec	13,685	9,405
<b>Total</b>	<b>1,547,708</b>	<b>1,080,364</b>

**Table 2:** Monthly energy consumption by Centrifugal Chiller

Months	Hours/day	TRH	kWh
Jan	4	124	1,978
Feb	6	168	5,204
Mar	13.5	420	18,925
Apr	17.2	516	22,115
May	22.8	707	45,855
Jun	24	720	71,140
July	23.7	734	91,654
Aug	24	744	81,567
Sep	23.5	705	70,296
Oct	23	713	47,225
Nov	10	300	7,677
Dec	3.3	103	1,956
<b>Total in lakh</b>			<b>4.66</b>

**Table 3:** Monthly Billing of PNG for year 2015

	Apr	Jun	Jul	Oct
Consumption	24,108	36,232	41,198	42,558
Price/scm	48.92	47.61	47.1	47.5
Consumption Value	1,179,362	1,725,004	1,940,424	2,021,504
Discount	36,162	54,348	61,796	63,836
VAT	57,160	83,532	93,930	97,882
<b>Total</b>	<b>1,200,360</b>	<b>1,754,188</b>	<b>1,972,558</b>	<b>2,055,550</b>

**Fig. 7.** PNG Consumption chart

## 5. RESULTS

Cost comparison of Trigen Plant and conventional screwed chiller has been carried out for the month of April, June, July & October for the year 2015 and the results are shown in the form of charts. The results shows that the trigen plant is no more economical than the conventional chiller plant. This is because due to the price hike in PNG. At the time of installation AIIMS claim the annual saving of about Rs2crore from this project because at that time the price of PNG was Rs16scm but in 2015 the price of PNG was about Rs47scm. They don't get the PNG at subsidized rate hence the running cost of trigen plant was increased gradually.

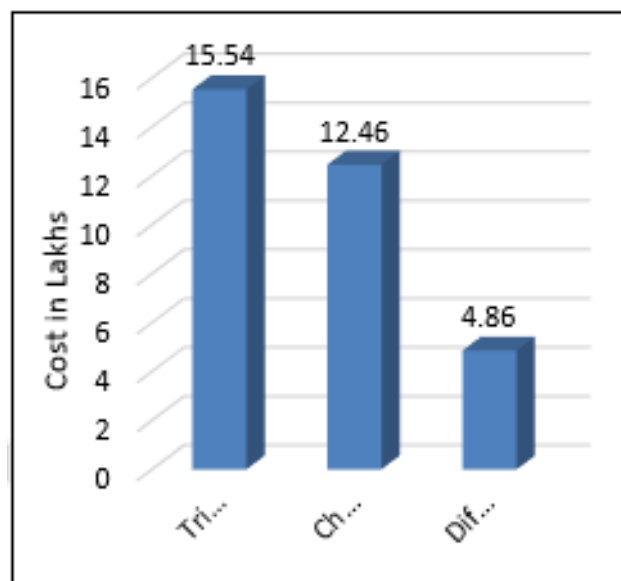


**Fig. 8.** Comparison result for April 2015

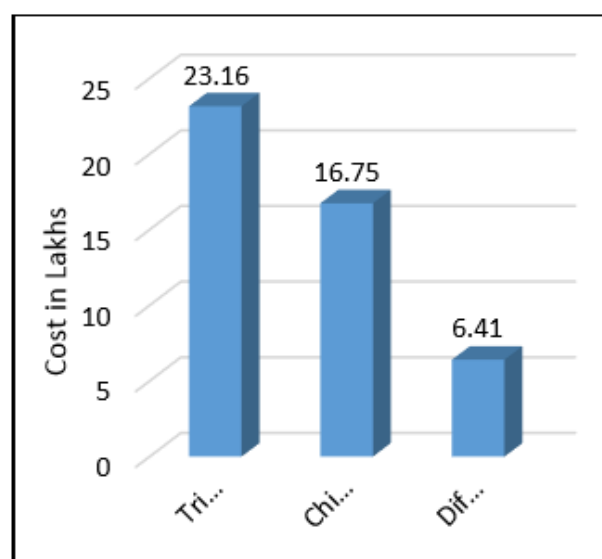


**Fig. 9.** Comparison result for June 2015

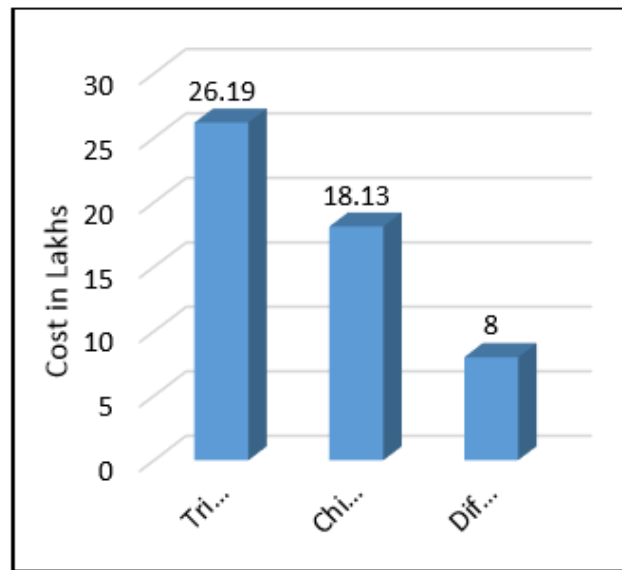


**Fig. 10.** Comparison result for July 2015

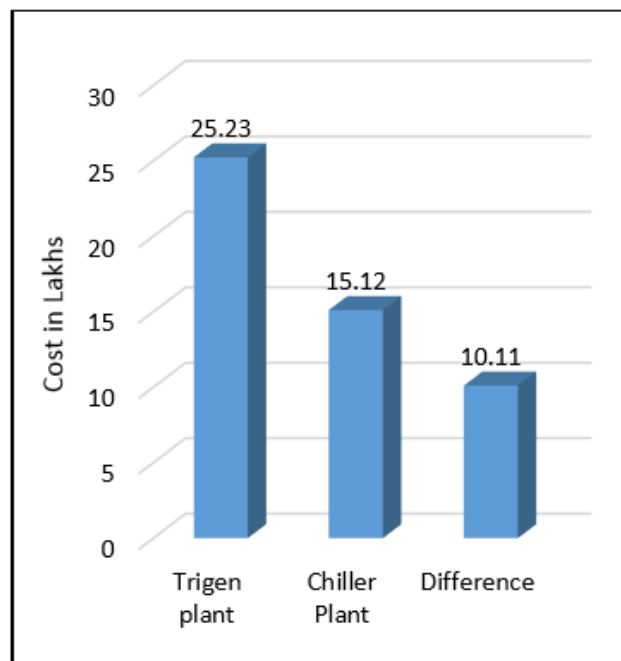


**Fig. 11.** Comparison result for October 2015

## 6. CONCLUSION

In this study performance assessment of a vapour absorption system based on waste heat plant and its comparison to the conventional chiller plant in operation for the duration of 2015 is presented. The VAM plant provides the air conditioning and chilled water plant to the JPNATC, AIIMS, New Delhi. The trigen plant includes DG set, VAM of cooling capacity 105TR and centrifugal chiller of 250Tr. The findings and suggestions are

1. The trigen plant is no more economical compare to conventional electrical chiller because of PNG price hike. If the trauma centre get the PNG at subsidized rate, the PNG plant will again run in profit.
2. The VAM does not run at the time of base load demand because the heat required by the VAM is produced when the DG set run at full load.
3. An idea is suggested to run the VAM at the time of base load demand by providing the additional heat by direct burning of PNG and regulating the flow of PNG by electronic controlled flow valve.

## NOMENCLATURE

TR = Tons of Refrigeration

AIIMS = All India Institute of Medical Sciences

JPNATC = Jai Prakash Narayan Apex Trauma Centre

AC = Air Conditioning

DG = Diesel Generator

VAM = Vapour Absorption Machine

scm = Standard Cubic Metre

CHW = Chilled Water

IGL = Indraprastha Gas Limited

NDMC = New Delhi Municipal Corporation

PNG = Piped Natural Gas

TRH = Total Running Hours

## REFERENCES

1. B.B. Saha, S. Koyama, T. Kashiwagi, A. Akisawa, K.C. Ng, H.T. Chua (2003), "Waste heat driven dual-mode, multi-stage, multi-bed regenerative adsorption system", *International Journal of Refrigeration*, Volume 26, Pages 749–757.
2. B.B. Saha \*, A. Akisawa, T. Kashiwagi (2001), "Solar/waste heat driven two-stage adsorption chiller: the prototype", *Renewable Energy*, Volume 23, Pages 93–101.
3. Ahmed Hamza H. Ali a, Peter Noeres, Clemens Pollerberg (2008), "Performance assessment of an integrated free cooling and solar powered single-effect lithium bromide-water absorption chiller", *Solar Energy*, Volume 82, Pages 1021–1030.
4. S. Mekhilef, R. Saidurb, A. Safari (2011), "A review on solar energy use in industries", *Renewable and Sustainable Energy Reviews*, Volume 15, Pages 1777–1790.
5. O. Marc, F. Lucas, F. Sinama, E. Monceyron (2010), "Experimental investigation of a solar cooling absorption system operating without any backup system under tropical climate", *Energy and Buildings*, Volume 42, Pages 774–782.
6. Y.L. Liu, R.Z. Wang, Z.Z. Xia (2005), "Experimental study on a continuous adsorption water chiller with novel design", *International Journal of Refrigeration*, Volume 28, Pages 218–230.
7. K. Balaji, R. Senthil Kumar (2012), "Study of Vapour Absorption System Using Waste Heat in Sugar Industry", *IOSR Journal of Engineering*, Volume 2, Issue, Pages 34–39.
8. B.B. Saha, S. Koyama, J.B. Lee, K. Kuwahara, K.C.A. Alam, Y. Hamamoto, A. Akisawa, T. Kashiwagi (2003), "Performance evaluation of a low-temperature waste heat driven multi-bed adsorption chiller", *International Journal of Multiphase Flow*, Volume 29, Pages 1249–1263.
9. Parfait Tatsidjodoung, Nolwenn LePierres, Lingai Luo (2013), "A review of potential materials for thermal energy storage in building applications", *Renewable and Sustainable Energy Reviews*, Volume 18, Pages 327–349.
10. A. Syed, M. Izquierdod, P. Rodrigueze, G. Maidment, J. Missenden, A. Lecuona, R. Tozerb (2005), "A novel experimental investigation of a solar cooling system in Madrid", *International Journal of Refrigeration*, Volume 28, Pages 859–871.
11. R.Z. Wang, T.S. Ge, C.J. Chen, Q. Ma, Z.Q. Xiong (2009), "Solar sorption cooling systems for residential applications: Options and guidelines", *International journal of refrigeration*, Volume 32, Pages 638–660.
12. R.Z. Wang, R.G. Oliveria (2005), "Adsorption refrigeration – An efficient way to make good use of waste heat and solar energy", *International sorption Heat Pump Conference*, June 22–24.
13. A. Elsafty, A.J. Al-Daini (2002), "Economical comparison between a solar-powered vapour absorption air-conditioning system and a vapour compression system in the Middle East", *Renewable Energy*, Volume 25, Issue 4, Pages 569–583.
14. Z.F. Li, K. Sumathy (2000), "Technology development in the solar absorption air-conditioning systems", *Renewable and Sustainable Energy Reviews*, Volume 4, Pages 267–293.
15. M. Balghouthi, M.H. Chahbani, A. Guizania (2008), "Feasibility of solar absorption air conditioning in Tunisia", *Building and Environment*, Volume 43, Issue 9, Pages 1459–1470.
16. Clito F.A. Afonso (2006), "Recent advances in building air conditioning systems", *Applied Thermal Engineering*, Volume 26, Issue 16, Pages 1961–1971.
17. Tiago Mateusa, b, Armando C. Oliveiraa (2009), "Energy and economic analysis of an integrated solar absorption cooling and heating system in different building types and climates", *Applied Energy*, Volume 86, Issue 6, Pages 949–957.
18. Constantinos A. Balarasa, Gershon Grossmanb, Hans Martin Henningc, Carlos A. Infante Ferreirad, Erich Podessere, Lei Wangd, Edo Wiemken (2009), "Solar air conditioning in Europe—an overview", *Renewable and Sustainable Energy Reviews*, Volume 11, Pages 299–314.
19. Nelson Fumo, D. Y. Goswami (2002), "Study of an Aqueous Lithium Chloride Desiccant System: Air Dehumidification and Desiccant Regeneration" *Solar Energy* Volume 72, Issue 4, Pages. 351–361.
20. R.B. Lokapure, J.D. Joshi (2012), "Waste Heat Recovery through Air Conditioning System" *International Journal of Engineering Research and Development*, Volume 5, Issue 3, Pages. 87–92.
21. S. Manojprabhakar, R.C. Ravindranath, R.V. Vinothkumar, A. Selvakumar, K. Visagave (2014), "Fabrication and Testing of Refrigeration Using Engine Waste Heat", *International Journal of Research in Engineering and Technology*, Volume: 03 Special Issue: 11



# Optimization of Surface Grinding Parameters for Flat Surface of AISI D3 using RSM

Umesh Kumar Vates\* Gyanendra Kumar Singh, Vivek Kumar, Shubham Sharma

Department of Mechanical Engineering,  
Amity School of Engineering & Technology, Amity University Uttar Pradesh, Noida, India

## **ABSTRACT**

*Conventional surface grinding is one of the most important machining processes, which is being used for surface finishing operations in manufacturing sector. Surface roughness ( $R_a$ ) and material removal rate (MRR) are the two major outputs to be considered during the surface grinding process. Response Surface Methodology (RSM) is used to investigate the effects of three controllable input variables namely-grit size, feed rate and depth of cut on  $R_a$  & MRR. Horizontal spindle surface grinding machine was used in order to conduct the experiment on die & tool steel (AISI D3) work piece. Central Composite Design (CCD) is used to performed  $L_{20}$  experimental design. Second-order polynomials regression equations are developed to predict the  $R_a$  and MRR within the experimental values and also check the adequacy of these models. Correlation coefficients ( $R^2$ ) were observed 96.05 % and 94.57 % for MRR and SR respectively. The responses were predicted as 0.0847g/min (MRR) & 1.2075 microns ( $R_a$ ) respectively using critical values of significant variables through RSM.*

**Keywords:** Grinding, Surface Roughness; Material Removal Rate, Response Surface methodology, Central composite design.

## **1.0 INTRODUCTION**

Conventional surface grinding process is frequently used in various industries from more than fifteen decades. Lot of surface finishing processes is being used to fulfill the industrial demand and customer satisfaction. In present scenario, most of the manufacturing industry demands for a high precision and more productivity at the same time. For the above purpose many attempts have been made by the researchers for modeling and optimization of grinding process to enhance the surface quality and MRR. Combined responses,  $R_a$  and MRR are still challenging problems. Pawan Kumar et al. (2015) studied the effect of abrasive tools on EN 24 steel surface using three parameters viz. grinding wheel speed of 850 RPM, table speed of 15m/min and depth of cut of 11.94 micrometer. The work was done on a surface grinding machine and optimizes the surface roughness and material removal rate using RSM technique. The predicted values were almost similar to the experimental values with  $R^2$  of 0.9164 for surface roughness and  $R^2$  of 0.99 for material removal rate. The error among predicted and



experimental values at the combination of all the input parameters for MRR and SR lie within 4.96% and 4.30% respectively. *B. Dasthagiri et al. (2015)* investigates the parameters such as cutting speed, feed rate and depth of cut influences the MRR and SR of mild steel and this was optimized using Response Surface Methodology model and tested through F-test and Analysis of Variance (ANOVA). *Lijohn et al. (2013)* presents the influence of input machining parameters as work speed, depth of cut and hardness of material on the surface roughness of various alloy steel materials such as EN 24, EN 31 and EN 353 using Taguchi parametric optimization as the optimization technique. The experiments were done on cylindrical grinding machine with  $L_9$  orthogonal array. SJ-400 surface roughness tester was used to measure the surface roughness of the various alloy steel materials. *M. Melwin et al. (2014)* reports that with optimum grinding parameters such as wheel speed of 150 RPM, depth of cut of 0.02mm and 1 number of pass, OHNS steel produces good surface finish when it is machined on cylindrical grinding machine. Besides this, precise tolerance can be gained on OHNS steel during cylindrical grinding. In this process of cylindrical grinding, to achieve larger metal removal rate, an important role is played by the number of passes. *N. Mohan et al. (2008)* selected best feasible network of interactive parameters with learning rate, number of neurons in hidden layer and error goals were decided automatically to investigate their effect on surface roughness by developing the neural network and fuzzy based methodology. The network model was trained using back propagation algorithms. The experiment was carried out for grinding of alloy steel using a black carbide silicon grinding wheel on traverse cylindrical grinding machine. He has considered only five controllable parameters in the grinding process to develop neural network model. The accuracy can be increased by indulging some other controllable parameters like dressing depth and dressing lead etc. *N. Alagumurthi, et al. (2006)* investigates that the input parameters like depth of cut, wheel speed & work speed play a major role in the quality of surface during grinding. It may be opted for the most suitable Design of Experiment to perform the work. As it verdict that the work speed has more influence on surface roughness and suggested that the factorial method is flexible, so it is more advantageous over the Taguchi method as the development of mathematical models and regression models is not feasible with the Taguchi method. When there are only a few numbers of tests required then Taguchi method is efficient but when the interactions between the process variables are present then the factorial method is more efficient and systematic. The results obtained from the grinding cycle time indicate that we can get more productivity if the optimal condition obtained by Taguchi technique is applied. Good quality products are obtained if the use of optimal parameters obtained through the factorial method. *Suresh P. Thakor et al. (2014)* came out with the result of the cylindrical grinding process using the signal-to-noise ratio approach, regression analysis approach for EN8 steel, the value of surface roughness and MRR water soluble oil as the cutting fluid is the most influencing parameter followed by work piece speed as 120 RPM and high depth of cut of 500 micrometer. Successful verification of optimum cutting parameters, full

factorial method was used for the conformation test for surface roughness and material removal rate. When water soluble oil was used as the cutting fluid with the higher work piece speed and higher depth of cut, an improved surface finish was obtained after grinding. *P. Vinay et al. (2015)* did experiment to get the better set of cutting forces and surface finish by doing the experiment under two different conditions, dry as well as pool cooling conditions and it was found that the AISI D3 yields good surface finish of 0.14 microns when dry grinding is done keeping low feed, low depth of cut and low dressing depth. *T. Mahajan et al (2015)* proposes that the table speed has the major effect on the surface roughness whereas depth of cut has the major effect on MRR of the surface grinding of AISI D2 steel. It was found that for minimum surface roughness the optimized parameters were wheel grit size (46) grinding wheel speed (2300), table speed (0.834), depth of cut (0.05). On the other hand, for maximum MRR, the optimized parameters were wheel grit size (36), grinding wheel speed (1650), table speed (0.834) and depth of cut (0.075). The optimized minimum surface roughness is 0.438 micrometer and maximum MRR is 60.231. *G. Manimaran et al. (2013)* conducted experiments on AISI 316 stainless steel using hydraulic surface grinder under three different grinding environments. It was found that the grey relational analysis and the Taguchi method are useful techniques for the optimization of multi response problems. Grinding under cryogenic cooling has more effect than conventional cooling. It was proved from the ANOVA testing those environments, DOC and work speed are influencing factors which has an impact on grinding of AISI 316 stainless steel. The effect of environment was 45.38% followed by work speed 29.41 % and DOC 15.52 %. It was suggested that the Taguchi-Grey technique can be applied to improve the grinding performance and the application of cryogenic cooling in the manufacturing industries. It is verdict that the process variables like grit size of the grinding wheel depending on its hardness, feed rate and depth of cut are the most viable influencing parameters on  $R_a$  & MRR.

In present research, optimization of the critical influencing parameters is being done using response surface methodology (RSM). The compromise between  $R_a$  and MRR is needed in conventional surface grinding to produce the satisfactory quality of the product with adequate productivity per unit on AISI D3. It is verdict that, combined optimization of MRR and  $R_a$  of the AISI D3 in grinding processes is needed to be done to fulfill the customer demand & economic production. In this work, horizontal spindle and reciprocating table type surface grinder is used on AISI D3 steel work piece with an  $Al_2O_3$  abrasives with different grit size grinding wheels. The most influencing parameters grit size, depth of cut and feed rate are selected based on the literature survey, which directly influences on  $R_a$  and MRR.

## 2.0 EXPERIMENTATIONS AND METHODOLOGY

AISI D3 steel was chosen for machining due to its capability and desire application. Work piece faces (dimensions of 800mm x 150mm x 25mm) were used to surface finish with application of  $Al_2O_3$  grinding wheels on surface grinder. The horizontal spindle and reciprocating table surface grinding machine was applied to do the tests. The compositions of work material AISI D3 and properties of  $Al_2O_3$  grinding wheels are illustrated in Table 1 & 2. Different grit size abrasive grinding wheels are given as Fig 1, whereas machined work materials and grinding operations are mentioned in Fig 2 & Fig.3.

**Table 1:** Composition of AISI D3 Die Steel

<i>C</i>	<i>Si</i>	<i>Mn</i>	<i>P</i>	<i>S</i>	<i>Cr</i>	<i>Ni</i>	<i>Mo</i>	<i>Al</i>	<i>Cu</i>	<i>Zn</i>	<i>Fe</i>
2.06	0.55	0.449	0.036	0.056	11.09	0.277	0.207	0.0034	0.13	0.27	85

**Table 2:** Properties of  $Al_2O_3$  grinding wheels

<i>Manufacturer Identification Numbers</i>	<i>type of abrasive</i>	<i>Grit Numbers</i>	<i>hardness</i>	<i>porosity</i>	<i>bond materials (resinoid reinforced)</i>	<i>Manufacturer Identifier</i>
51	A	140	K	8	BF	5
51	A	100	K	8	BF	5
51	A	60	K	8	BF	5



White Aluminum Oxide



Brown Aluminum Oxide



Grey Aluminum Oxide

**Fig. 1.** Different grit size abrasive wheels



**Fig. 2.** AISI D3 material work piece



**Fig. 3.** Surface Grinder

## 2.1. Surface Roughness Measurements and MRR Calculation

Surface Roughness measurements were carried out using a portable stylus type profile-meter (Mitutoyo Surface Tester SJ-210). The profile-meter was set to a cut-off length of 0.8 mm, filter 2CR, and traverse speed 1mm/second and 4 mm evaluation length. Centre line average (CLA) values of surface roughness (SR) were measured in the transverse direction of work piece. The values of SR measurement were repeated three times for each reading and average value was recorded. The parameters that affect MRR and surface roughness are spindle speed, feed, coolant concentration and flow rate. Optimal parametric combination may deals the technological quality of a product, which mostly influence the manufacturing cost of the product. SR is defined as the arithmetic value of the profile from the centerline along the length. This can be express as

$$R_a = 1/L \int y(x) |dx| \quad (1)$$

Where L is the sampling length, y is the profile curve and x is the profile direction. The average 'R<sub>a</sub>' is measured within stylus travelling length of 0.8 mm. Centre-line average 'CLA' value of SR measurements were taken to provide quantitative evaluation of the effect of drilling parameters on surface finish. The average value of three reading up to two decimal place of microns will be obtained the least count 1nm (nanometer) as Fig.4.



**Fig. 4.** Surface roughness measuring instrument (SJ 210)

The amount of material removal was obtained by finding the weight difference before and after machining using a precision electronic digital weight balance with 0.1mg resolution. The MRR is calculated using the following formula:

$$\text{MRR (gram/sec)} = (W_i - W_f) / t \quad (2)$$

Where  $W_i$  is initial weight of workpiece in gram (before machining);  $W_f$  is final weight of workpiece in gram (after machining);  $t$  is machining time in seconds.

## 2.2. Response Surface Methodology

RSM is a collection of mathematical and statistical techniques that are useful for modeling and analysis of problems in which output or response is influenced by several input variables and the objective is to find the correlation between the response and the variables investigated. It is one of the Design of Experiments (DOE) methods used to approximate an unknown function for which only a few values are computed. These relations are then modeled by using least square error fitting of the response surface. A central composite design (CCD) is used since it gives a comparatively accurate prediction of all response variable averages related to quantities measured during experimentation. CCD offers the advantage that certain level adjustments are acceptable and can be applied in the two-step chronological RSM. In these methods, there is a possibility that the experiments will stop with few runs and decide whether the prediction model is satisfactory or not.

In CCD, the limits of the experimental domain to be explored are defined and are made as wide as possible to obtain a clear response from the model. The grit size, feed, depth of cut are the machining variables selected for this investigation. The different levels have been taken for this study which depicted in Table 3. An experiment in series of test called runs.  $L_{20}$  runs DOE at three levels were selected critically as per the feasibility and scope of setup. Material removal rate and surface roughness values are given in table 4 for 20 tests according to different control levels.

The second-order model is normally used when the response function is not known or nonlinear. In the present study, a second-order model has been utilized. The experimental values are analyzed and the mathematical model is then developed that illustrate the relationship between the process variable and response. The second-order model in equation 3 explains the behavior of the system.

$$y = a_0 + \sum_{i=1}^n a_i x_i + \sum_{i=1}^n a_{ii} x_i^2 + \sum_{i=1}^n \sum_{j=1, j \neq i}^n a_{ij} x_i x_j \quad (3)$$

Where Y is the corresponding response,  $X_i$  is the input variables,  $X_i^2$  and  $X_i X_j$  are the squares and interaction terms respectively, of these input variables.

**Table 3:** Factor and their levels for surface grinding of AISI D3

<i>Factor</i>	<i>Name</i>	<i>Units</i>	<i>Levels</i>		
			<i>-1</i>	<i>0</i>	<i>1</i>
A	Grit size	microns	80	120	150
B	Depth of cut	mm	0.2	0.4	0.6
C	Feed rate	mm/min.	0.5	1	1.5

**Table 4:** Experimental Observation.

S. No	Wheel Grit Size	Depth of Cut	Feed Rate	MRR (gm/sec)	Surface Roughness (Micron)
1	80	0.4	1	0.0645	1.052
2	150	0.4	1	0.094	2.263
3	120	0.6	1	0.1095	1.433
4	120	0.4	1	0.0776	1.56
5	120	0.4	0.5	0.0582	1.37
6	120	0.2	1	0.0619	1.82
7	120	0.4	1.5	0.0814	1.675
8	120	0.4	1	0.0822	1.423
9	150	0.2	0.5	0.0608	2.34
10	150	0.6	1.5	0.1471	2.113
11	120	0.4	1	0.0746	1.572
12	80	0.6	0.5	0.0513	0.976
13	120	0.4	1	0.0844	1.589
14	120	0.4	1	0.085	1.562
15	150	0.2	1.5	0.0966	2.744
16	120	0.4	1	0.0863	1.965
17	80	0.2	0.5	0.05	1.29
18	80	0.6	1.5	0.0744	1.25
19	150	0.6	0.5	0.1222	1.87
20	80	0.2	1.5	0.0566	1.323



### 2.3. Regression models

Based on the experimental data, statistical regression analysis enabled to study the correlation of process parameters with the MRR and SR. Both linear and non-linear regression models were examined and verdict based on high to very high coefficients of correlation ( $R^2$ ) calculated. In this study, three variables are under consideration to obtain the polynomial regression modeling. For simplicity, a quadratic model of MRR and  $R_a$  are proposed. The effects of these variables and the interaction between them were included in this analysis's as Fig.5 & Fig.6 respectively. The coefficients of regression model of  $R_a$  & MRR are estimated from the experimental data as presented in Table 5 & 6. The standard errors on estimation of the coefficients are tabulated in the column 'MRR coefficient' and ' $R_a$  coefficient'. The P & T values are calculated for 95% level of confidence and the factors having p-value more than 0.05 are considered insignificant (shown with \*\* in p-column). Model adequacy was also tested as per the present residuals as represented in Fig.7. The model made to represent MRR and  $R_a$  depicts that grit size, feed, feed<sup>2</sup>, and interaction of grit size and depth of cut are most influencing parameters in order of significance. The final response equation for MRR and  $R_a$  are non-linear in nature, a linear polynomial will not be able to predict the response accurately. Therefore the second-order model (quadratic model) is found to be adequate for the grinding process.

**Table 5:** Estimated Regression Coefficients for  $R_a$  (micron)  
Estimated Regression Coefficients for  $R_a$  (microns)

Term	Coef	SE Coef	T	P
Constant	1.50778	0.05058	29.808	0.000**
Grit Size (microns)	0.54390	0.04573	11.894	0.000**
Depth of cut (mm)	-0.18495	0.04575	-4.043	0.002**
Feed rate (mm/min.)	0.12466	0.04575	2.725	0.021
Grit Size (microns)*	0.18363	0.08927	2.057	0.067
Grit Size (microns)				
Depth of cut (mm)*Depth of cut (mm)	0.07118	0.08720	0.816	0.433
Feed rate (mm/min.)*	-0.03282	0.08720	-0.376	0.715
Feed rate (mm/min.)				
Grit Size (microns)*	-0.08910	0.05102	-1.746	0.111
Depth of cut (mm)				
Grit Size (microns)*	0.04327	0.05102	0.848	0.416
Feed rate (mm/min.)				
Depth of cut (mm)*	0.01000	0.05113	0.196	0.849
Feed rate (mm/min.)				

S = 0.144607

PRESS = 0.825054

R-Sq = 94.57%

R-Sq (pred) = 78.57%

R-Sq (adj) = 89.68%

Algorithm to find the  $R_a$ .

$R_a$  (microns) =  $1.71601 - 0.0163186a - 0.984612b + 0.187505c + 0.000149902a^2 + 1.77955b^2 - 0.131273c^2 - 0.0127287ab + 0.00247276ac + 0.100000bc$

**Table 6:** Estimated Regression Coefficients for MRR  
Estimated Regression Coefficients for MRR (g/sec)

Term	Coef	SE Coef	T	P
Constant	0.076787	0.002353	32.636	0.000**
Grit Size (microns)	0.02239	0.002127	10.527	0.000**
Depth of cut (mm)	0.017524	0.002128	8.235	0.000**
Feed rate (mm/min.)	0.011249	0.002128	5.286	0.000**
Grit Size (microns)*	0.004861	0.004152	1.171	0.269
Grit Size (microns)				
Depth of cut (mm)*Depth of cut (mm)	0.008014	0.004056	1.976	0.076
Feed rate (mm/min.)*	-0.007886	0.004056	-1.944	0.08
Feed rate (mm/min.)				
Grit Size (microns)*	0.011764	0.002373	4.957	0.001
Depth of cut (mm)				
Grit Size (microns)*	0.003868	0.002373	1.63	0.134
Feed rate (mm/min.)				
Depth of cut (mm)*	0.0007	0.002378	0.294	0.775
Feed rate (mm/min.)				

S = 0.00672616

PRESS = 0.00405301

R-Sq = 96.05%

R-Sq(pred) = 64.60% R-Sq(adj) = 92.49%

Algorithm to find the MRR.

$$\text{MRR (g/sec)} = 0.104189 - 0.00116629a - 0.272921b + 0.0573730 + 3.96851E-06a^2 + 0.200341b^2 - 0.0315455c^2 + 0.00168059ab + 0.000221016ac + 0.00700000bc$$

The ANOVA for the curtailed quadratic model depicts the value of coefficient of determination of MRR and  $R_a$  are  $R^2$  as 96.05% and 94.57%, which signifies that how much variation in the response is explained by the model. The higher of  $R^2$ , indicates the better fitting of the model with the data. However,  $R^2_{adj}$  is 92.49% and 89.68% which accounts for the number of predictors in the model describes the significant coefficient relationship. It is important to check the adequacy of the fitted model, because an incorrect or under-specified model can lead to misleading conclusions. By checking the fit of the model one can check whether the model is under specified. The model adequacy checking includes the test for significance of the regression model, model coefficients, and lack of fit, which is carried out subsequently using ANOVA on the curtailed model. The total error on regression is sum of errors on linear, square, and interactions terms. The residual error is the sum of pure and lack-of-fit errors. The fit summary recommended that the quadratic model is statistically significant for analysis of SR. In the table, p-value for the lack-of-fit is 0.186, which is insignificant, so the model is certainly adequate. Moreover, the mean square error of pure error is less than that of lack-of-fit.



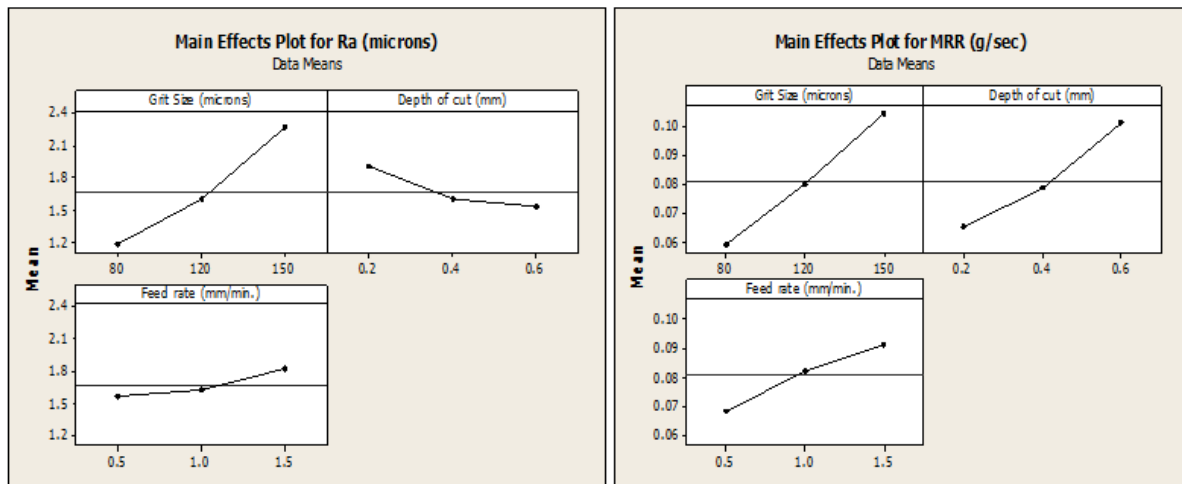


**Fig. 5.** Main effect plot for  $R_a$  & MRR with significant control variables

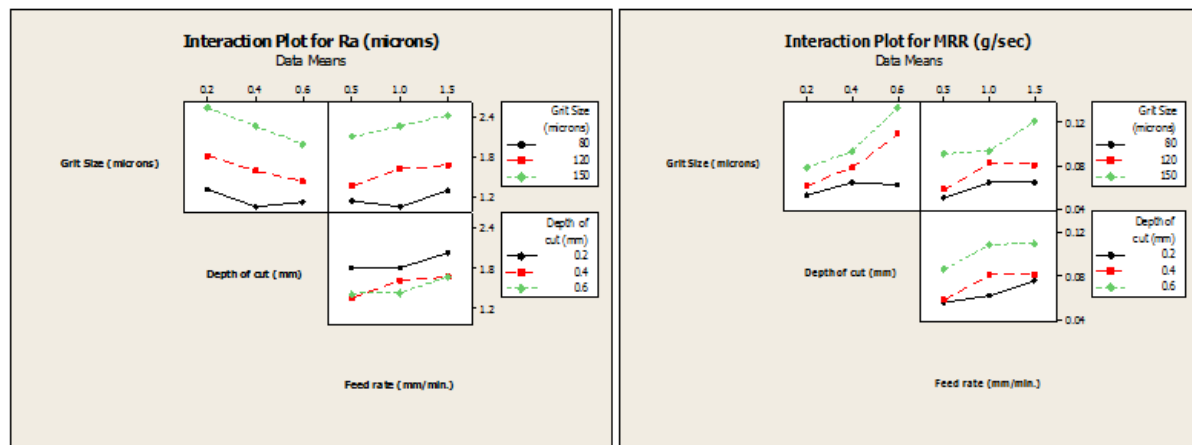


**Fig. 6.** Interactions plot for  $R_a$  & MRR with significant control variables

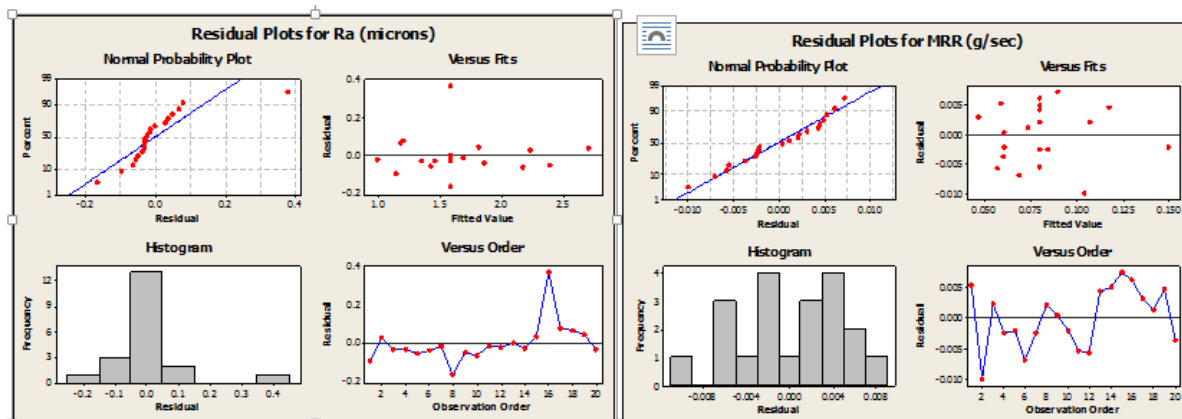


**Fig. 7.** Residual plot for  $R_a$  & MRR

### 3.0 RESULT AND DISCUSSION

It is very clear that surface roughness is minimum at certain input parametric combinations & other hand MRR also maximum at same combinations. It is very difficult to obtain such influencing parametric combinations which applicable to achieve the optimal responses as surface roughness and material removal rate. Lot of modeling and optimization techniques are frequently used in the grinding processes for different materials, but the RSM is the most important for modeling and optimization tool which applicable for the multi objective response optimization. The responses  $R_a$  & MRR have successfully predicted up to the adequate level 1.2075 microns & 0.0847 g/sec at combination of variable as grit size (92.7273), depth of cut (0.60) & feed rate (1.1465) using multi objective response optimization technique as Fig.8.

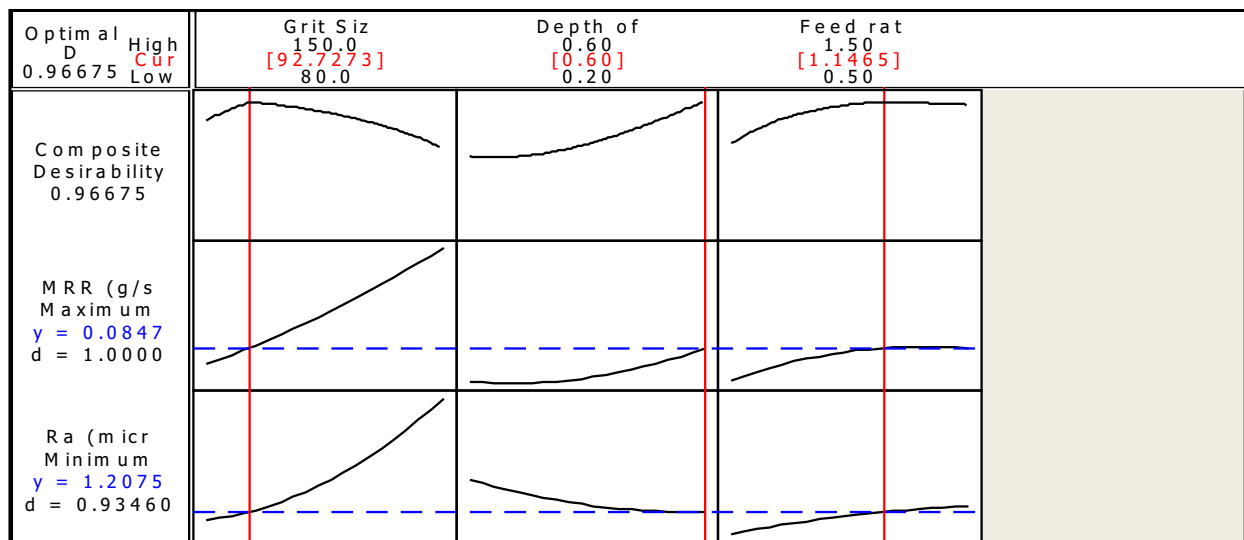


**Fig. 8.** Response optimization plot ( $R_a$  & MRR)

The effect of the machining parameters (grit size, feed and depth of cut) on the response variables MRR & SR have been predicted. It can be seen from the Fig.9, the MRR tends to increase significantly with increase in feed rate & depth of cut for any value of grit size. However, the  $R_a$  tends to decrease significantly with decrease in feed rate & grit size for any value of depth of cut.

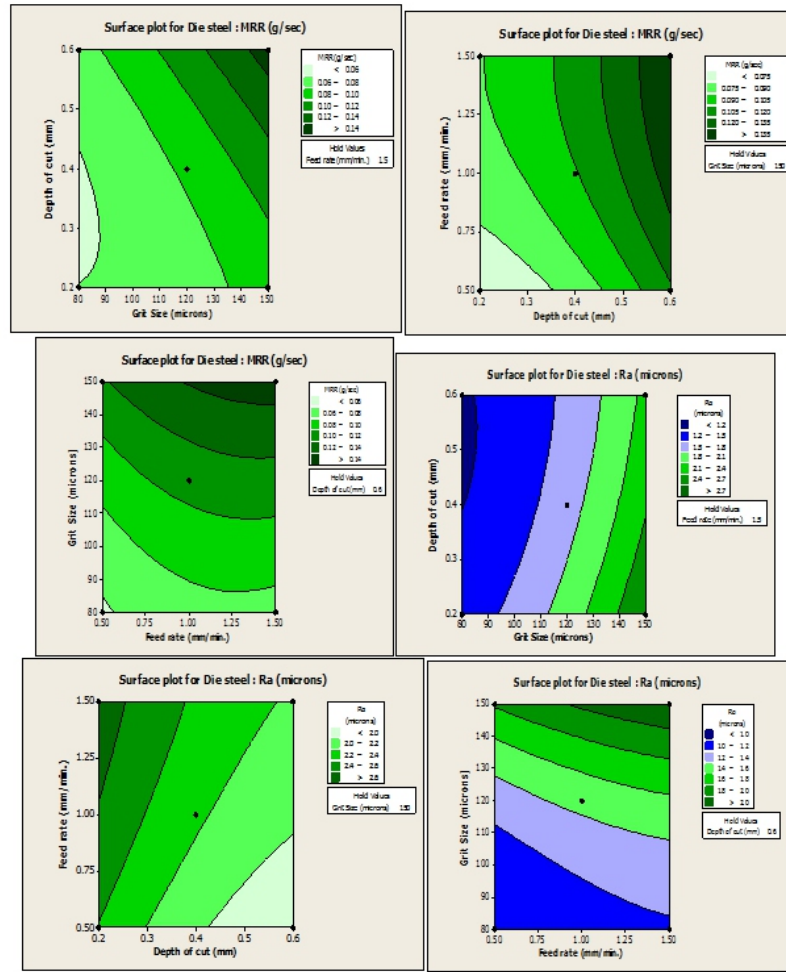


**Fig. 9.** Effect of two variables at a time with  $R_a$  & MRR

## 4.0 CONCLUSIONS

In the present study, the process parameters are significantly influencing on  $R_a$  and MRR. A second order response model of these parameters are developed and found that grit size, feed, speed<sup>2</sup> and interaction of speed\* feed and grit size\*depth of cut with other parameters significantly affects the  $R_a$  & MRR. RSM techniques were also implemented to predict the  $R_a$  and MRR. Correlation coefficient ( $R^2$ ) values were observed 96.05 % and 94.57% for MRR and  $R_a$  respectively. The responses have predicted as 1.2075 microns & 0.0847 g/min at combination of variable as grit size (92.7273), depth of cut (0.60) & feed rate (1.1465). This research can also help for the researchers' and industries personal to prediction the  $R_a$  & MRR within the experimental range, without performing the experiments using RSM model.

## REFERENCES

1. Alagumurthi, N; 'Optimization of Grinding Process through Design of Experiment (DOE) – A Comparative Study'. *Material and Manufacturing Processes*, pp; 19-21 (2006).
2. Dasthagiri, B.; Goud, E.V.G; 'Optimization Studies on Surface Grinding Process Parameters' *International Journal of Innovative Research in Science Engineering and Technology*. Vol.4 (7), pp; 6148-6156 (2015).
3. George, L.P; Job, V.K.; Chandran, I.M; 'Study on Surface Roughness and its Prediction in Cylindrical Grinding Process based on Taguchi Method of Optimization'. *International Journal of Scientific and Research Publications* Vol.3 (5), pp; 1-5 (2013).
4. Kumar, P; Kumar, A.; Singh, B; 'Optimization of Process Parameters in Surface Grinding using Response Surface Methodology' *International Journal of Research in Mechanical Engineering & Technology*, Vol.3 (2), pp; 245-252 (2013).
5. Mahajan, T.V; Nikalje, A.M; Supale, J.P; 'Optimization of Surface Grinding Process Parameters for AISI D2 steel, *International Journal of Engineering Sciences and Research Technology*. Vol.4 (7), pp; 944-949 (2015).
6. Manimaran, G.; Kumar, M.P 'Multi response Optimization of Grinding AISI 316 Stainless Steel Using Grey Relational Analysis' *Materials and Manufacturing Process*. Vol 28 (4), pp; 418-423; (2013).
7. Selvan, M.C.P; Raju, N.M.S; 'Assessment of Process Parameters in Abrasive Water jet Cutting of Stainless Steel'; *International Journal of Advances in Engineering & Technology* Vol.1 (3).pp; 34-40 (2011).
8. Sridhar, M.M.J; Manickam, M; Kalaiyarasan, V; 'Optimization of Cylindrical Grinding Process Parameters of OHNS Steel (AISI 0-1) Rounds Using Design of Experiment Concept'. *International Journal of Engineering Trends and Technology*.Vol. 17 (3), pp; 109-114 (2014).
9. Thakor, S.P; Patel, D.M; 'An Experimental Investigation on Cylindrical Grinding Process Parameters for EN 8 using Regression Analysis, *International Journal of Engineering Development and Research* Vol.2(2),.pp; 2486-2491 (2014)..
10. Vinay, P.V; Rao, C.H; 'Experimental Analysis and Modeling of Grinding AISI D3 Steel' *International Journal of Recent Advances in Mechanical Engineering* Vol.4 (1), pp; 47-60 (2014).

# A Review on Room Temperature Magnetic Refrigeration for Domestic Applications

Mohammad Talha Javed<sup>a</sup>, Naved Azum<sup>b\*</sup>

<sup>a</sup>Department of Mechanical Engineering, Faculty of Engineering and Technology, Jamia Millia Islamia, New Delhi, India

<sup>b</sup>Chemistry Department, King Abdul Aziz University, Jeddah, Saudi Arabia

## **ABSTRACT**

*Room Temperature Magnetic Refrigeration is a highly efficient, eco friendly and safe technology which although is not fully mature but serves as a viable alternative for vapor compression refrigeration technology. In this paper, magneto caloric effect which forms the basis of this technology has been discussed. Furthermore, different types of magneto-caloric materials, thermodynamics related to magnetic refrigeration, magnetic field generation and different magnetic refrigeration prototypes have been discussed.*

**Keywords:** *Magneto-caloric Effect, Magneto-caloric Material, Room Temperature Magnetic Refrigeration, Room Temperature*

## **1. INTRODUCTION**

The ever increasing demand in cooling has resulted in high usage of refrigeration and air conditioning based on vapor compression technology. 17% of the electricity produced in the world is used up in cooling. Vapor compression technology uses chlorine and fluorine based refrigerants. These refrigerants are the main source of ozone depletion as laid down in the Montreal protocol. Furthermore, the use of compressors in vapor compression technology makes the process considerably inefficient. The use of chlorine and fluorine based refrigerants also increases the operating and maintenance cost as leakage of refrigerant in gaseous state is inevitable. These disadvantages compelled the scientists and researchers to search for a better cooling technology. Room temperature magnetic refrigeration (RTMR) is an emerging cooling technology which is a promising alternative for the existing vapor compression technology. Magnetic refrigeration works on the principle of magnetocaloric effect. RTMR is an environment friendly cooling technology which has a number of excellent features[7,8,9]such as:

- ❑ Compact configuration
- ❑ Low noise and vibrations
- ❑ High efficiency( Energy saving upto 50 %)
- ❑ Low maintenance ( Reduced Operating cost )
- ❑ High stability
- ❑ Better Reliability
- ❑ Non polluting ( No effluents )

As a result, RTMR has been one of the trending field of research in the world. Currently, it has been recognized as one of the nine advanced subjects of the International Institute of Refrigeration (IIR).

## 2. SYSTEM DESCRIPTION

A magnetic refrigerator consists of the following basic components:

1. Magnetocaloric material: It forms the core of the magnetic refrigerator and is the working material.
2. Magnet: Magnet or magnets capable of producing high field in the range of 1 T to 7 T are required.
3. Working fluid: Working fluid performs the function of transfer of heat from hot and cold sources. Generally a water based fluid is used.

Fig. 1 shows the working of a simple magnetic refrigeration system.

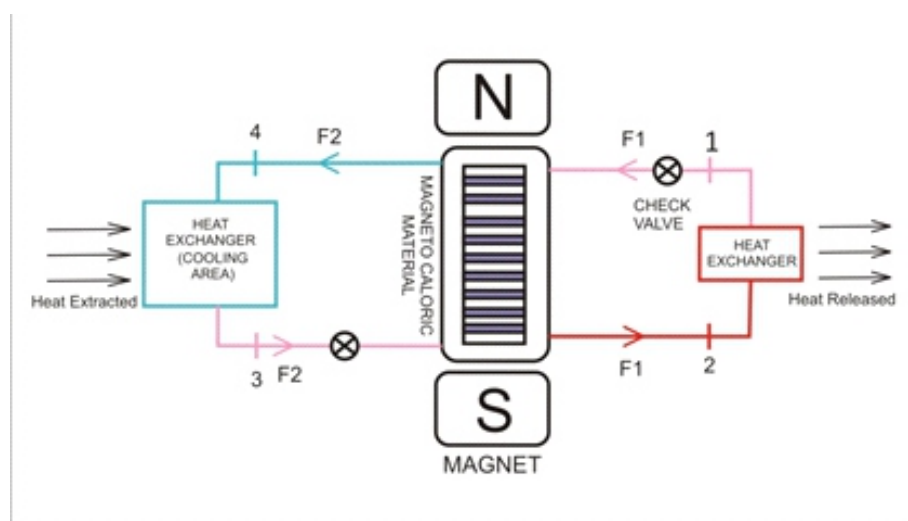


**Fig. 1.** Schematic Diagram of a Magnetic Refrigerator

Process 1-2 : Magnetic field is turned on and the temperature of MCM increases. Fluid F1 enters MCM through check valve and extracts heat from it at  $T_c$ . F1 is pumped to a heat exchanger where it expels heat to the surrounding.

Process 3-4 : Magnetic Field is turned off and the temperature of MCM decreases . Fluid F2 enters MCM through the second check valve and gives away heat. F2 is pumped to the second heat exchanger and extracts heat from the cooling area.

### 3. LITERATURE REVIEW

This work is a review of development in the area of Room Temperature Magnetic Refrigeration. The articles of study can be classified into the following areas :

1. Magnetic Materials: These articles deal with the research done on materials suitable for RTMR. The properties of such materials and feasibility for use in a RT magnetic refrigerator has been discussed
2. Thermodynamic analysis: These articles deal with the thermodynamic aspect of magnetic refrigeration technology.
3. Magnets: There are a few research papers dealing with the type and form of magnetic field which can be used in RTMR.
4. Magnetic refrigerator Prototypes: These articles includes the different types of magnetic refrigerator prototypes built till date.

### 4. MATERIALS

#### *4.1 Criteria for selecting magneto-caloric material*

A number of factors affect the selection of magneto caloric substance for room temperature magnetic refrigeration. The selection of magneto caloric material has to be done by considering the following properties[61,10, 76]:

- Large magneto caloric effect ( Large magnetic entropy change and large adiabatic temperature change )
- Large density of magnetic entropy
- Small lattice entropy
- Modest Curie temperature in the vicinity of working temperature to guarantee that the large magnetic entropy change can be obtained in the whole temperature range of the cycle;
- No magnetic hysteresis losses

- Low thermal hysteresis losses
- Small specific heat and large thermal conductivity ( to ensure remarkable temperature change and effective heat transfer )
- Large electrical resistance and thereby low eddy current losses
- High chemical stability and inertness
- Low cost and availability
- Easy to synthesize

#### *4.2 Magnetocaloric materials*

A number of MCM have been studied by different researchers till date. Gd is considered to be the prototype material Later on different alloys of Gd were studied Different MCM have been studied and those suitable for magnetic refrigeration have been listed down. MCM can be broadly classified into the following categories:

1. Gd and its alloys
2. Perovskite and perovskite-like compounds
3. Transition metal compounds
4. Composite material

##### *4.2.1 Gd and its alloys*



**Table 1:** Review of Gd and its alloy

Name and Title	Year	Magnetic material	T <sub>C</sub> (K)	ΔH (T)	ΔS <sub>M</sub> (J kg <sup>-1</sup> K <sup>-1</sup> )	Remarks
Dan'kov SY et al, Magnetic phase transitions and the magneto thermal properties of gadolinium	1998	Gd	294	1.5	3.8	Temperature change rate ? 6K/T. Suitable for RTMR
				3	7.1	
				5	10.2	
				6	11.4	
Dai W et al, . New magnetic refrigeration materials for temperature range from 165 K to 235 K.	2000	Gd <sub>0.5</sub> Dy <sub>0.5</sub>	230	5	10.2	(Gd,Dy) <sub>1-x</sub> Ndx ( x =0, 0.1, 0.2, 0.3) alloys have been studied and Gd <sub>0.5</sub> Dy <sub>0.5</sub> is found suitable.
Pecharsky VK et al, The influence of magnetic field on the thermal properties of solids.	2010	Gd <sub>0.74</sub> Tb <sub>0.26</sub>	280	5	11.5	Suitable for RTMR
Canepa F et al, . Magnetocaloric properties of Gd <sub>7</sub> Pd <sub>3</sub> and related intermetallic compounds	2002	Gd <sub>7</sub> Pd <sub>3</sub>	323	5	ΔT <sub>ad</sub> = 8.5 K	magnetocaloric properties of Gd <sub>7</sub> Pd <sub>3</sub> was obtained, ΔS <sub>M</sub> , ΔT <sub>ad</sub> and the refrigerant capacity Q. Found to be suitable.
Pecharsky VK et al, Tunable magnetic regenerator alloys with a giant magnetocaloric effect for magnetic refrigeration from ~20 K to ~290	1997	Gd <sub>5</sub> (Si <sub>x</sub> Ge <sub>1-x</sub> ) <sub>4</sub>				With change in the value of x, the MC properties changes. The most suitable compounds with respective x values have been studied.
		X=0.43	247	5	39	42
		X=0.5	276	5	18.4	
		X=0.505	280	5	11.7	
Pecharsky VK et al, The giant magnetocaloric effect in Gd <sub>5</sub> (Si <sub>x</sub> Ge <sub>1-x</sub> ) <sub>4</sub> materials for magnetic refrigeration	1998	Gd <sub>5</sub> (Si <sub>1.985</sub> Ge <sub>1.9</sub> <sub>85</sub> Ga <sub>0.03</sub> ) <sub>2</sub>	290	5	ΔT <sub>ad</sub> = 15K	The T <sub>C</sub> is easily tunable by changing the value of x and by alloying with Ga the T <sub>C</sub> reaches ~290 K (RT). This compound is found to be suitable for RTMR.

The lanthanide metal gadolinium (Gd) is the prototype magnetic material available for RTMR. It has a Curie temperature of 294 K at which it Gd undergoes a second-order paramagnetic ferromagnetic phase transition. The MCE [11-24] and the heat capacity [24-27] of Gd have been studied in many research activities. Its  $\Delta T_{ad}$  values at  $T_C$  are ~6, 12, 16, and 20 K for  $\Delta H=2, 5, 7.5$ , and 10 T, respectively; its  $\Delta S_M$  is about  $4.2 \text{ J kg}^{-1} \text{ K}^{-1}$  for  $\Delta H=1.5 \text{ T}$  at  $T_C$ . It has good thermal conductivity. It is the prototype material for laboratory research of MR. The only disadvantage it possess is that it easily oxidizes. Some Gd-based intermetallic compounds also to possess large MCE. Both  $\text{Gd}_{0.74}\text{Tb}_{0.26}$  [28] and  $\text{Gd}_{0.5}\text{Dy}_{0.5}$  [29] present the MCE equivalent to Gd at 280 K and at 265 K, respectively. Eutectic  $\text{Gd}_{76}\text{Pd}_{24}$  was found to have two  $\Delta T_{ad}$  peaks of 8.4 K and 9.4 K at 294 K and 323 K, respectively, and it is favorable to be used in magnetic Ericsson cycle because the adiabatic temperature change is almost constant in the room temperature range [30]. Reversible giant MCE in a series of GdSiGe alloys was observed in Ames Laboratory [32–34]. A lot of of research has been devoted to the this series [35–41,43]. These alloys have a first-order magnetic transition between 30 and 275 K depending on the Si to Ge ratio, and have peak values of magnetic entropy change 2–10 times larger than that of known prototype magnetic refrigerant materials. It is observed that the  $\Delta S_M$  values of the series of  $\text{Gd}_5(\text{Si}_x\text{Ge}_{1-x})_4$  alloys where  $0 \leq x \leq 0.5$ , are at least twice that of Gd. Furthermore, by alloying with Ga, the giant MCE temperature increases to ~290 K [32,33]. Although this series presents a number of favorable properties for RTMR, this series of metals have disadvantages such as easy oxidation, hard preparation, and high price, which needs to be resolved before they are applied in room temperature magnetic refrigeration.

#### 4.2.2 Perovskite and perovskite-like compounds

**Table 2:** Review of Pervoskite and perovskite-like compounds

Name and Title	Year	Magnetic Material	$T_c(K)$	$\Delta H(T)$	$\Delta S_M (J\ kg^{-1}\ K^{-1})$	Remarks
		$La_{1-x}Ca_xMnO_3$				
Guo ZB et al, Large magnetic entropy change in perovskite-type manganese oxides	1997	$x=0.2$	230	1.5	5.5	Large magnetic entropy change is observed due to anomalous thermal expansion at $T_c$ .
		$x=0.33$	267	3	6.4	
Bohigas X et al, Magnetocaloric effect in $La_{0.65}Ca_{0.35}Ti_{1-x}Mn_xO_3$ ceramic perovskites.	1999	$x=0.35$	255	3	5.2	Suitable for use in RTMR
Bohigas X et al, Tunable magnetocaloric effect in ceramic perovskites	1998	$x=0.4$	263	3	5	Suitable for RTMR
Chen W et al, Research on magnetocaloric effect of $La_{1-x}K_xMnO_3$ .	1998	$La_{0.9}K_{0.1}MnO_3$	283	1.5	1.5	Suitable for RTMR
Guo ZB et al, . Large magnetic entropy change in perovskite-type manganese oxides	1997	$La_{0.75}Ca_{0.15}Sr_{0.10}MnO_3$	327	1.5	2.8	Convenient for RTMR

Large magnetic entropy change has been found in the perovskite manganese oxides in recent years, thereby making these materials a contender for room temperature magnetic refrigeration. The main advantages of this series of compounds over Gd and GdSiGe alloys are low cost, non-active chemical property (no oxidation), little coercive force as well as high electric resistance. Many studies on these compounds have been completed and are currently under progress[44–60]. Their Curie temperature also can be easily tuned to the needed range by introducing specific metal additions. However,  $\Delta S_M$  will decrease much in the meantime, reducing their practicability. For example,  $\Delta S_M$  of  $La_{0.8}Ca_{0.2}MnO_3$  in the presence of 1.5 T magnetic field reaches  $5.5\ J\ kg^{-1}\ K^{-1}$ , about 1.5 times of Gd, but its Curie temperature is only 230 K. After adjusting Ca ratio to  $La_{0.6}Ca_{0.4}MnO_3$ , its Curie point increases to 263 K but  $\Delta S_M$  decreases to 70% of Gd at 3.0 T. To improve the Curie temperatures by adding Sr and Pb, the Curie temperatures reach 327 and 296 K, however  $\Delta S_M$  decreases again. In addition, the behavior of heat transfer of these compounds is not suitable because they are oxides. Table 2 describes the properties of few such materials.

### 4.2.3 Transition metal compounds

**Table 3.** Review of Transition metal compounds

Name and Title	Year	Magnetic material	T <sub>C</sub> (K)	ΔH (T)	ΔS <sub>M</sub> (J kg <sup>-1</sup> K <sup>-1</sup> )	Remarks
Hu FX et al, Magnetic entropy change in Ni <sub>51.5</sub> Mn <sub>22.7</sub> Ga <sub>25.8</sub> alloy	2000	Ni <sub>52.6</sub> Mn <sub>23.1</sub> Ga <sub>24.3</sub>	300	5	~18	MC properties were analysed. Found suitable for RTMR
Wada H et al, Giant magnetocaloric effect of MnAs <sub>1-x</sub> Sb <sub>x</sub>	2001	MnAs	318	5	30	Very large MCE observed at RT
Wada H et al, Extremely large magnetic entropy change of MnAs <sub>1-x</sub> Sb <sub>x</sub> near room temperature	2002	MnAs <sub>0.9</sub> Sb <sub>0.1</sub>	~286	5	~30	Extremely large MCE observed at RT
Tegus Q et al, Transition-metal-based magnetic refrigerants for room-temperature applications	2002	MnFeP <sub>0.45</sub> As <sub>0.55</sub>	300	5	18	Large MCE observed, found suitable for RTMR

Early in 1984, Oesterreicher observed the MCE effect of rare-earth transition metal compounds whose Curie temperatures are in the range of room temperature, and suggested that it is possible for the series of Y<sub>2</sub>Fe<sub>17-x</sub>Co<sub>x</sub> and Y<sub>2</sub>Fe<sub>17-x</sub>Ni<sub>x</sub> compounds to be room temperature magnetic refrigerants [61]. The maximum ΔT<sub>ad</sub> in the series of Ce<sub>2</sub>Fe<sub>17-x</sub>Co<sub>x</sub> and Er<sub>2</sub>Fe<sub>17-x</sub>Ni<sub>x</sub> (x=0.3–2.0) are 4.75 and 4.51 K (in a 2 T magnetic field), and their corresponding Curie temperature values are 294.2 K and 293.5 K, respectively, comparable to the metal Gd but is much less expensive than Gd [62]. Hence, this series of compounds are of vital practical application. The non-rare-earth alloys of Ni-Mn-Ga undergo a first order transition, which brings about a great magnetic entropy change [63,64]. The magnetic entropy change of Ni<sub>52.6</sub>Mn<sub>23.1</sub>Ga<sub>24.3</sub> at 300 K is ~18.0 J kg<sup>-1</sup> K<sup>-1</sup> which exceeds that of Gd near room temperature [63]. It has a range of only few K and there is a 6 K thermal hysteresis accompanying the transition, which make this alloy unfavorable. Among the transition-metal-based compounds, MnAs shows a giant MCE. It has a Curie Temperature of 318 K and the magnetic entropy change induced by a 5 T magnetic field is 30 J kg<sup>-1</sup> K<sup>-1</sup> at T<sub>c</sub> but the magnetic transition is accompanied by a large thermal hysteresis [65]. The ΔS<sub>M</sub> of MnAs<sub>1-x</sub>Sb<sub>x</sub> for 0 ≤ x ≤ 0.3 in a 5 T field reaches 25–30 J kg<sup>-1</sup> K<sup>-1</sup>, and the presence of Sb for As can tune the Curie temperature between 230 K and 315 K without considerable reduction of ΔS<sub>M</sub>. Other than that there is no hysteric behavior for 0.05 ≤ x. These materials are also less costly than other materials [66]. Another compound MnFeP<sub>0.45</sub>As<sub>0.55</sub> exhibits a giant magnetic entropy change comparable to the giant MCE material Gd<sub>5</sub>Ge<sub>2</sub>Si<sub>2</sub>. Variation of the P/As ratio between 3/2 and 1/2 tunes the T<sub>C</sub> and the optimal operating temperature between 200 and 350 K, without losing the giant MCE [67]. Table 3 shows the properties of some compounds of this family at varying parameters.

### 4.2.4. Composite material

**Table 4:** Review of Composite Materials

Name and Title	Year	Material	Remark
Hashimoto T et al, A new method of producing the magnetic refrigerant suitable for the Ericsson magnetic refrigeration.	1987	$\text{ErAl}_{2.2}$ , $\text{HoAl}_{2.2}$ , $(\text{Dy}_{0.5}\text{Ho}_{0.5})\text{Al}_{2.2}$ and $\text{DyAl}_{2.2}$	Four given materials were used to form a composite to be used in RTMR. $\Delta T$ obtained for Ericson cycle = $\sim 15$ K
Hashimoto T et al, New application of complex magnetic materials to the magnetic refrigerant in an Ericsson magnetic refrigerator	1987	$(\text{ErAl}_2)_{0.312}(\text{HoAl}_2)_{0.198}(\text{Ho}_{0.5}\text{Dy}_{0.5}\text{Al}_2)_{0.490}$	Composite material suitable for RTMR is analyzed for a Rankine Cycle.
Chahine R. et al, Composite materials for Ericssonlike magnetic refrigeration cycle	1997	$\text{Gd}_{1-x} - \text{Dy}_x$	Two sets of composite materials proposed with $\Delta S_{\text{COM}} = 8$ and $7.3$ J/K.gK
		(with $x = 0, 0.12, 0.28, 0.49$ , and $0.70$ )	

A single material may possess the problem of insufficient operating range for RTMR to compensate the needs of ideal magnetic Ericsson cycle. In such cases a method of composition was first raised by Brown [75] in which a few ferromagnetic materials with different magnetic phase transition temperature  $T_c$  are composed to form one new material whose  $\Delta S_M$  is even in the range of refrigeration temperature. Tokyo Institute of Technology have made experimental trials to make the layer structural sintered material composed of ErAl, HoAl, (DyHo)Al and DyAl alloys in the low temperature range [68,69]. In a separate investigation, two sets of composite materials were obtained with the temperature range of 240 – 290 and 210 – 290 K, respectively from the GdDy alloys. Constant  $\Delta S_M$  of 8.0 and 7.3 J kg<sup>-1</sup> K<sup>-1</sup> in the required temperature range are obtained[70]. Nanometer-sized magnetic materials may be a useful option for future application [71–75].

## 5 THERMODYNAMICS

**Table 5.** Review of Thermodynamics Related To Magnetic Refrigeration

Name and Title	Year	Subject	Remarks
Debye P et al, Comments on magnetization at low temperature	1926	Magnetocaloric Effect and Magnetic Refrigeration	An overview of Magnetic Refrigeration is present in the paper
Giauque WF et al, . A thermodynamic treatment of certain magnetic effects. A proposed method of producing temperatures considerably below 1 absolute	1927	Magnetocaloric Effect and Magnetic Refrigeration	Method of producing very low temperatures using MCE is devised
Pecharsky VK et al, . Magnetocaloric effect from indirect measurements: magnetization and heat capacity	1999	MCE properties	$\Delta S_M$ , $\Delta T_{AD}$ and Heat Capacity variation and relation for MCE is analyzed
Pecharsky VK et al, Some common misconception concerning magnetic refrigerant materials	2001	MCE properties	The relationships between the isothermal entropy change and the adiabatic temperature change, respectively, have been analyzed.
Osterreicher et al, ., Magnetic cooling near Curie Temperature above 300 K	1984	MCE and Magnetic Refrigeration	Magnetic cooling of different MC materials near Curie Temperature above 300 K are studied.
Cross CR et al, Optimal temperature-entropy curves for magnetic refrigeration	1988	T-S curves	Optimal T-S diagrams for magnetic refrigerators using Carnot, Ericsson and Brayton cycles were determined and compared to results of thermodynamic numerical models
Yan ZJ et al, The characteristic of polytropic magnetic refrigeration cycles.	1991	Thermodynamic cycles for magnetic refrigeration	The concepts of polytropic refrigeration cycles, which consist of two isothermal processes and two generalized polytropic processes of paramagnetic salt, are introduced
Dai W et al, Regenerative balance in magnetic Ericsson refrigeration cycles	1992	Thermodynamic cycles for magnetic refrigeration	The coefficient of performance of the refrigeration cycles of ferromagnetic material is derived
Lixuan Chen et al, characteristics of a Brayton refrigeration cycle of paramagnetic salt	1994	Magnetic Brayton cycle	The characteristics of a magnetic Brayton refrigeration cycle are investigated on the basis of the general equation of state of a simple paramagnetic salt
Zhengrong Xia et al, Performance analysis and parametric optimal criteria of an irreversible magnetic Brayton-refrigerator	2008	Magnetic Brayton Cycle	An irreversible magnetic Brayton refrigeration-cycle model is established, in which the thermal resistance and irreversibility in the two adiabatic processes are taken into account and performance characteristics are investigated

### 5.1 Magneto caloric effect

Warburg was the first person to discover magnetocaloric effect in iron in 1881 [1]. The fundamental principle governing the magnetocaloric effect was suggested by P. Debye(1926) and W. Giauque (1927) [2,3]. The first fully functional prototype of magnetic refrigerator was built by Brown in 1976. MR technology was first successfully applied in low temperature magnetic refrigeration (Cryogenics).

MCE arises due to the coupling of the magnetic sub lattice with the magnetic field, which changes the magnetic entropy ( magnetic part of entropy ) of the solid. When a magnetic field is applied to paramagnetic and soft ferromagnetic materials, their magnetic moments gets aligned and ordered. Thereby the magnetic entropy decreases and heat is released by the material. When the magnetic field is reduced isothermally the magnetic moments again becomes disordered, the magnetic entropy increases and the material absorbs heat [4]

The entropy of a magnetic solid,  $S(T,H)$ , at constant pressure (which is a function of both the magnetic field strength ( $H$ ) and the absolute temperature ( $T$ )), is the sum of the magnetic entropy,  $S_M$  and lattice entropy,  $S_{LAT}$  :

$$S(T,H) = S_M(T,H) + S_{Lat}(T)$$

Fig 1 depicts the behavior a MC material. It shows the adiabatic temperature change involved in magnetocaloric effect between the presence and absence of magnetic field. A zero magnetic field  $H_0$  and a non zero magnetic field  $H_1$  are applied on a ferromagnetic material. When the magnetic field is applied adiabatically the magnetocaloric effect (i.e. the adiabatic temperature rise,  $T_{ad} = T_1 - T_0$ ) can be observed as the isentropic difference between the corresponding  $S(T)_H$  functions[5].



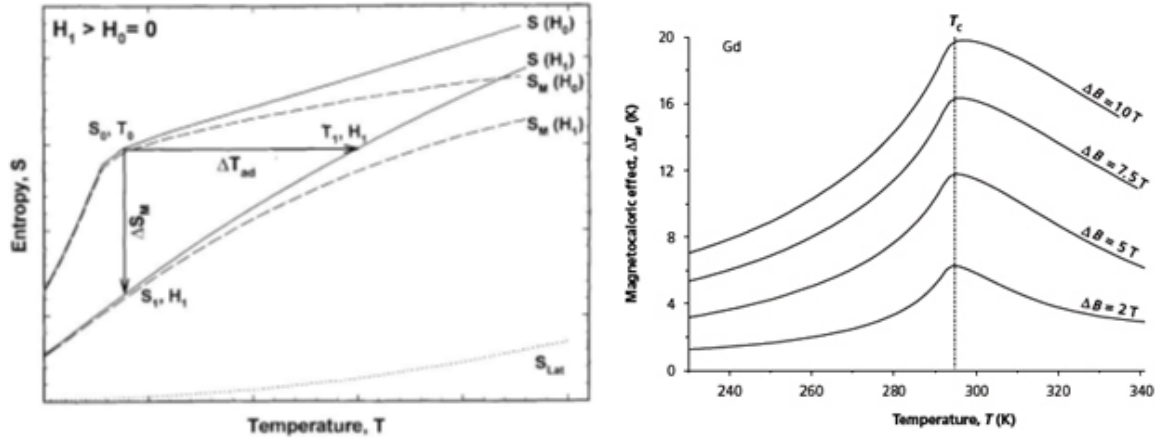


**Fig. 2.** (a) Characteristics of a MCM in presence and absence of magnetic field, (b) Variation of magnetocaloric effect with temperature

Thereby, it is observed that application of magnetic field brings about change in temperature of a paramagnetic and simple ferromagnetic material at constant entropy.  $\Delta H$  must be maximized in order to maximize the MCE [6]

## 5.2 Magnetic refrigeration cycle

Magnetic refrigerator achieves cooling/refrigeration using a magnetic material through magnetic refrigeration cycle. Magnetization and demagnetization helps achieve cooling, and two other required processes. The basic cycles for magnetic refrigeration are magnetic Carnot cycle, magnetic Stirling cycle, magnetic Ericsson cycle and magnetic Brayton cycle, among which the magnetic Ericsson and Brayton cycles are applicable for room temperature magnetic refrigeration. Ericsson and Brayton cycles employ a regenerator to achieve a large temperature span and are easy to operate

### 5.2.1 Magnetic Ericsson cycle

Ericsson cycle consists of two isothermal processes/ stages and two isofield processes as illustrated in Fig5 The cycle illustrates the ther modynamic property of the magnetic refrigerant.

1. Isothermal magnetization process [(A→B in Fig. 2(a)) : The magnetic field increases from  $H_0$  to  $H_1$ . The heat is transferred from magnetic refrigerant to upper regenerator fluid,  $Q_{ab} = T_1(S_a - S_b)$ , which makes the upper fluid increase in temperature.
2. Isofield cooling process [B→C in Fig. 2(a)) : In constant magnetic field of  $H_1$ , both magnetic refrigerant and electromagnet move downward to bottom and hence heat  $Q_{bc} = S_c \int_{S_b}^{S_b} T dS$  is transferred from magnetic refrigerant to upper regenerator fluid.

3. Isothermal demagnetization process III[C→D in Fig. 2(a)] When magnetic field decreases from  $H_1$  to  $H_0$ , the magnetic refrigerant absorbs heat  $Q_{cd} = T_0(S_d - S_c)$  from the lower regenerator fluid. After that, the fluid decreases in temperature.
4. Isofield heating process [D→A in Fig. 2(a)] In the field of  $H_0$ , magnetic refrigerant and electromagnet move upward to the top and the lower regenerator fluid absorbs heat  $Q_{da} = \int_{S_a}^{S_d} T dS$ .

For getting the maximum efficiency or the efficiency of magnetic Carnot cycle, it is required in the Ericson cycle, that the heat transferred in the two isofield processes  $Q_{bc}$ ,  $Q_{da}$  are equal. Ericson cycle exhibits optimal performance with refrigerants having parallel T-S curves.[77 - 82].

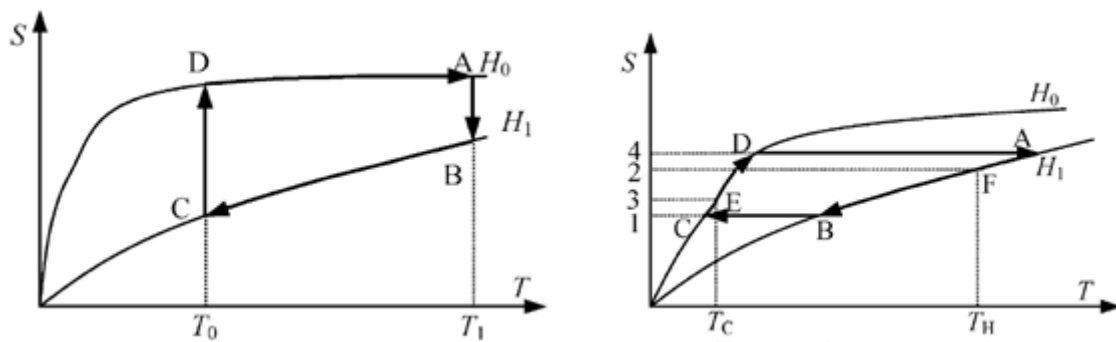


**Fig 3.** (a) Magnetic Ericson cycle, (b) Magnetic Brayton Cycle

### 5.2.2 Magnetic Brayton cycle

Magnetic Brayton cycle consists of two adiabatic processes and two isofield processes as shown in Fig.6 The magnetic refrigerant forms a cycle between the magnetic field of  $H_0$  and  $H_1$ , and the high and low temperature heat source  $T_H$  and  $T_C$ , respectively.

1. Isofield cooling process : A→B (constant magnetic field of  $H_1$ ): magnetic refrigerant expels heat to the first working fluid as Fig. 6 indicates.
2. Adiabatic demagnetization B→C : Magnetic Field is removed adiabatically and no heat flows in or out of the magnetic refrigerant.
3. Isofield Heating C→D (constant magnetic field  $H_0$ ): magnetic refrigerant absorbs heat from the second working fluid.
4. Adiabatic Magnetization D→A : No heat flows into or out of the magnetic refrigerant during the adiabatic magnetization process.

The Brayton cycle can exhibit optimal performance with magnetic refrigerants having parallel T–S curves [77, 83-85].

## 6 MAGNETIC FIELD

**Table 6.** Review of Magnetic field applicable in a magnetic refrigeration system

Name and Title	Year	Subject	Remarks
Casas-Cubillos J et al, M. A pulsed superconducting magnet for a static magnetic refrigerator operating between 1.8K and 4.5K	1994	Superconducting magnet for magnetic refrigerator	In the framework of development for an industrial-size 1.8 K magnetic refrigerator using a static active material, a pulsed superconducting magnet producing up to 3 T at a ramping rate of 6.5 T/s is designed, built and tested
Rowe JR et al, Conductively cooled Nb <sub>3</sub> Sn magnet system for a magnetic refrigerator	1991	Magnet for magnetic refrigerator	A Nb <sub>3</sub> Sn magnet system for use in a magnetic refrigerator has been developed and tested
Trueblood JR et al, A vertically reciprocating NbTi solenoid used in a regenerative magnetic refrigerator	1991	Magnet for magnetic refrigerator	An 8.2T-NbTi superconducting solenoid used for periodic magnetization by vertical motion along a bed of magnetocaloric material in a regenerative magnetic refrigerator using all active magnetic regenerator (AMR) has been designed, fabricated, and tested
Osterreicher H et al, Magnetic cooling near Curie temperature above 300K	1984	Adiabatic temperature change for varying magnetic fields	Different MC materials have been analyzed and variation of temperature and magnetic entropy with magnetic field has been studied.

The magnetic field is one of the most important parameters to be considered in RTMR. There are two modes to apply magnetic field on magnetic refrigerant:

- (a) Both magnetic refrigerant and magnet are static. Pulsed magnetic field [86] or alternate on-off magnetic field is applied. There is no driving device and power consumption is high.
- (b) There is relative movement between magnet and magnetic refrigerant. The movement may either be reciprocating [87] or rotary [88].

The specific MCE rate change at  $T \approx T_C$  is  $\sim 3$  K/T at lower fields and  $\sim 2.2$  K/T at higher fields.[22]. The adiabatic temperature change  $\Delta T_{ad}$  is approximately proportional to the magnetic field  $H^{2/3}$ [61]. Generally, both superconductor cooled by liquid-helium and electromagnet can supply a 5–7 T high fields.

## 7 ACTIVE MAGNETIC REGENERATIVE REFRIGERATION (AMRR)

**Table 7.** Review of Magnetic Regenerators

Name and Title	Year	Subject	Remarks
Engelbrecht, K.L. et al, Modeling Active Magnetic Regenerative Refrigeration Systems	2005	Magnetic regenerator	Modeling of a magnetic regenerator
Tura A. et al, Design and testing of a permanent magnet magnetic refrigerator.	2007	Magnetic regenerator in a magnetic refrigerator	A refrigerator with AMRR is tested
Matsumoto K et al, thermodynamic analysis of magnetically active regenerator from 30 to 70 K with a Brayton-like cycle	1990	Magnetic regenerator	A model active regenerator with a Brayton-like operation cycle was analyzed by numerical cycle simulation
Degregoria AJ. Et al, Modeling the active magnetic regenerator	1992	Active magnetic regenerator	A time-dependent one-dimensional model of the Active Magnetic Regenerator (AMR) is described
Pecharsky VK et al, Magnetocaloric effect and magnetic refrigeration.	1999	Review on magnetic refrigeration	Magnetic regenerator is discussed as a part of review

Existing MCE materials do not achieve high temperature differences which makes it difficult for them to be used at RT [89]. For example, a sample of gadolinium around room temperature produces an MCE of approximately 10 K in a magnetic field of 5 T. Thus it is difficult to use such MCE materials in RTMR [90].

This technical barrier has been overcome by the application of the Active Magnetic Regenerative Refrigeration (AMRR) [89,90,91]. In such systems the heat rejected by the network in one step of the cycle is restored and returned to the network in another step of the cycle [96]. The regenerative bed consists of plates of MCE material. The bed itself acts as a regenerator. The different solid parts of the regenerator are connected by the fluid. The steps in AMRR can be categorized as follows :

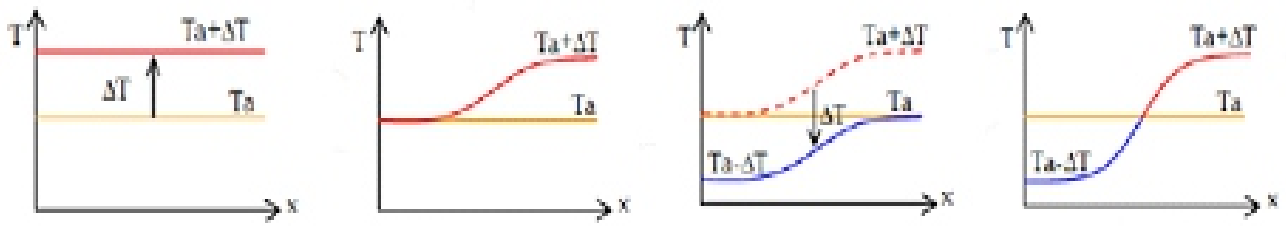


**Fig. 4.** (a) Step 1, (b) Step 2, (c) Step 3, (d) Step 4

1. Magnetization of material from an initial state when the system is at temperature  $T_a$ . The temperature of the regenerator increases by  $\Delta T$ .
2. Fluid flows from a cold source  $T_c$  to hot source  $T_h$  and takes away heat from the regenerator. This creates a temperature gradient along the bed.
3. Demagnetization of the material takes place and the temperature of the regenerator falls by  $\Delta T$ .
4. The fluid now flows from the hot source to the cold source and transfers its heat to the regenerator.

Each particle of the bed undergoes a regenerative Brayton cycle (93). This cycle is repeated 'n' times and the  $\Delta T$  generated is amplified at each cycle to reach the temperatures limits of hot and cold sources (steady state). The  $\Delta T$  obtained in the process is higher than the adiabatic temperature change  $\Delta T_{ad}$  (MCE)[93,94].

## 8 MAGNETIC REFRIGERATOR PROTOTYPES

**Table 8.** Review of Magnetic Refrigerator Prototypes

Name and location	Year	Type and max. frequency (Hz)	Max. cooling Power (W)	Max. $\Delta T$ (K)	Max. magnetic field strength (T)	Magnetocaloric regenerator material
<a href="#">Brown (1976, 1978)</a> NASA, USA	1976	Reciprocating		47 (80)	Supercond. 7	1 mm Gd plates, 20% ethyl alcohol- water
<a href="#">Kirol and Dacus (1987)</a> Idaho National Engineering Laboratory, USA	1987	Rotating type, Ericsson cycle 0.5 Hz		11	Permanent 0.9 T	125 Gd plates 76 mm, spacing 127 mm, water
<a href="#">Zimm et al. (1998)</a> AMES Ast. Corp. A., USA	1997	Reciprocating	600	38	Supercond. 5	Gd spheres 0.15e0.3 mm
<a href="#">Okamura et al. (2005)</a> Tokyo Inst. Tech Chubu Electric Power, Japan	2000	Reciprocating	100	21	Supercond. 4	Gd spheres
<a href="#">Zimm et al. (2003, 2005, 2006)</a> , Astronautics Corp. America, Madison, Wisconsin, USA	2001	Rotary 4 Hz	50	25	Permanent 1.5	Gd, GdEr spheres, 0.25-0.5 mm, water with inhibitors
<a href="#">Okamura et al. (2005)</a> Tok. Inst. Tech. Chubu Electric Japan	2003	Rotary (rotation of magnets) 0.4 Hz	60	8	Permanent 0.77	Gd <sub>1-x</sub> Dy <sub>x</sub> layered alloys, spheres 0.6 mm, 1 kg, water
<a href="#">Okamura et al. (2007)</a> Tokyo I. Tech., Chubu Electric Power, Japan	2005	Rotary	110	10	Permanent 0.77	Gd alloys MnAsSb alloys, and Gd packed beds Water
<a href="#">Vasile and Müller (2005, 2006)</a> INSA, Cooltech Applications Strasbourg, France	2005	Rotary	360	14	Permanent 2.4	Gd plates, water
<a href="#">Yao et al. (2006)</a> Technical Institute of Physics and Chemistry, Beijing, China	2006	Reciprocating 1 Hz	51	42	Permanent 1.5	Gd particles, helium
<a href="#">Okamura et al. (2005, 2007)</a> Tokyo Inst. Tech., Chubu Electric Power, Japan	2006	Rotary 0.5 Hz	560	8	Permanent 1.1	Gd foils, water
<a href="#">Huang et al. (2006, 2007)</a> Baotou Research Institute of Rare Earth, China	2006	Reciprocating	50	18	Permanent 1.5	Gd 750 g and LaFe <sub>10.97</sub> Co <sub>0.78</sub> Si <sub>1.05</sub> B <sub>0.2</sub> 200 g, alkaline water solution, Ph ¼ 10
<a href="#">Zimm et al. (2007)</a> Astronautics Corp. America Madison, Wisconsin, USA	2007	Rotary 4 Hz	220	12	Permanent 1.5	Gd plates, water
<a href="#">Buchelnikov et al. (2007)</a> Chelyabinsk State University Russia	2007	Rotary 10 Hz	40		Permanent 1	Gd, NiMnGa alloys
<a href="#">Tura and Rowe (2009)</a> University of Victoria, Victoria, Canada	2009	Rotary 4 Hz	50	29	Permanent 1.4	Gd spheres, 300 mm

### 8.1 The magnetic system of Brown

Brown developed a rotating system which employs an Ericsson cycle [98]. The magnetic field is produced by an electromagnet (water cooled) with a maximum magnetic field of 7 T. Gd is used as the magnetocaloric material in the form of plates with 1 mm thickness, separated by stainless steel wires with 1 mm intervals to allow the regenerator fluid to flow vertically. The fluid used is a mixture of 80% water and 20% alcohol. The working body is held stationary in the magnetic field while the regenerator tube containing the fluid, oscillates up and down. The 7-T field is turned on and off at appropriate time during the cycle to complete the demagnetization cooling isofield (zero field), magnetization heating and isofield (strong field) processes sequentially. Without load and after 50 cycles, the temperatures reached were  $46^{\circ}\text{C}$  for the heat source and  $-1^{\circ}\text{C}$  for the cold source, thus  $\Delta T = 47^{\circ}\text{C}$ . However, the cooling capacity is unremarkable as a result of a larger temperature span. Moreover, the cycle could not be operated quickly and the temperature gradient decreased both for the easy mixing between high- and low-temperature fluid in regenerator.

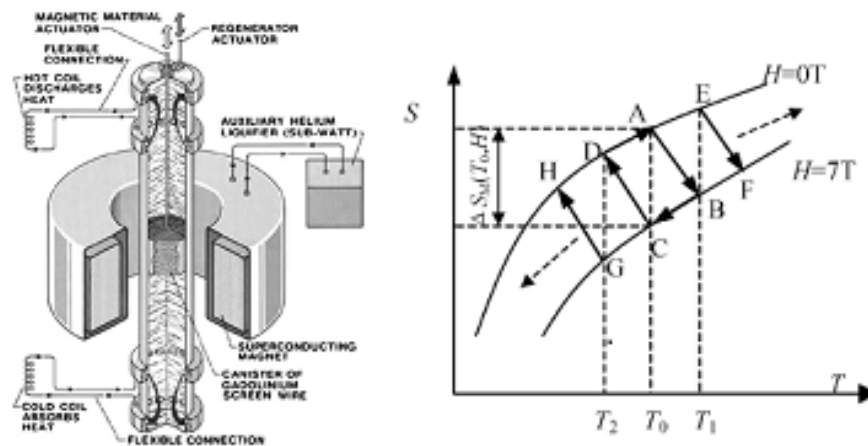


**Fig. 5.** (a) Brown's Magnetic Refrigerator construction, (b) Brown's Magnetic Refrigerator thermodynamic cycle

### 8.2 The magnetic system of Steyert

Steyert designed a system with a rotating refrigerant, implementing a Brayton's cycle [99, 100]. In this system, the porous magnetocaloric material rotates across high and low fields as shown in Fig. 9. The fluid enters the wheel (regenerator) at the temperature  $T_{\text{hot}}$  and exits at the temperature  $T_{\text{cold}}$ , during which it transfer its heat energy to the magnetic material in the low field region. After receiving the heat from the load ( $Q_{\text{cold}}$ ) the fluid enters the wheel again at a temperature  $T_{\text{cold}} + \Delta$  and receives heat from the

magnetic material to attain a temperature  $T_{\text{hot}} + \Delta$  in the high field region. Finally, the fluid transfers heat  $Q_{\text{hot}}$  to a reservoir and the fluid is again pumped back to complete the cycle.

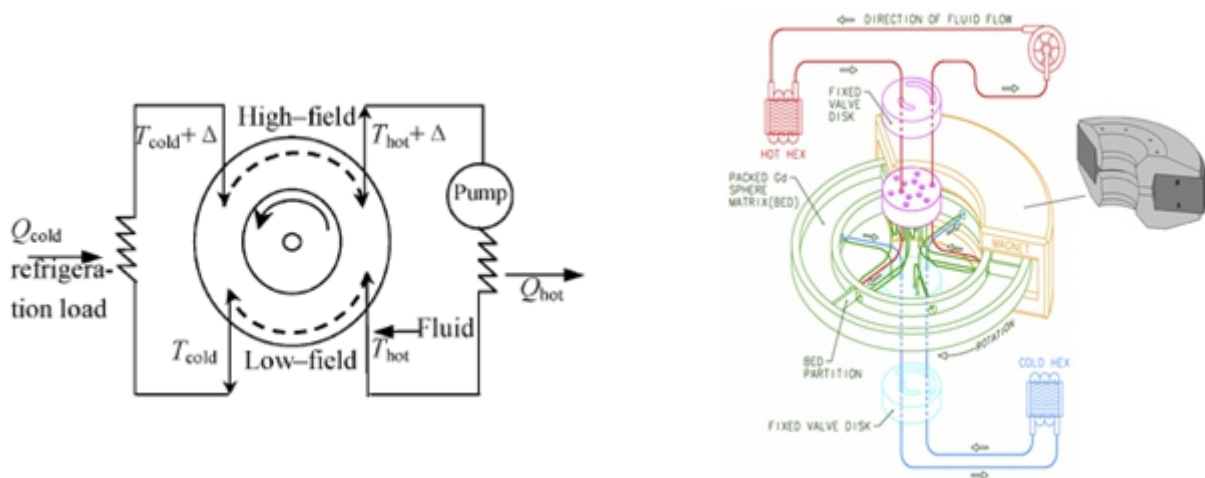


**Fig. 6.** (a) magnetic system of Steyert, (b) Magnetic System of Zimm

### 8.3 The magnetic system of Zimm

This magnetic refrigerator developed by Zimm [101] is reciprocating type in accordance with the magnetic Brayton cycle. The. An AMRR system was designed; it consists of a wheel with 6-bed regenerators composed of gadolinium powder. This wheel is rotating inside an area of high magnetic field of 5 T. The heat transfer fluid is water (added with antifreeze). The flow of the fluid is adjusted according to the relative position of each bed inside the magnetic field. Fig. 8 shows the photography of this prototype. The results show that in a 5 T field, it can generate up to 600 W of cooling power and its efficiency approaches 60% of Carnot with a COP approaching 15 but with increasing temperature span to about 38 K cooling power falls to about 100 W. It can still generate about 200 W cooling power in a 1.5 T magnetic field. Moreover, the device has been operated for more than 1500 h and 18-month period without any major maintenance or any breakdowns.

### 8.4 Cooltech systems

Between the years 2011 to 2016 received a number of patents [105,106,42] for magnetic refrigerator prototypes developed by them. Cooltech appliances worked towards the industrialization and commercialization of an integrable magnetic refrigeration system and in 2015 they came up with their first commercial product. This refrigeration system can be retrofitted or integrated with any commercial refrigerator of comparable capacity. This product is now available in the market with a cooling capacity in the range of 200-700 W . Temperatures of about 2 – 5°C were attained during tests of this product.



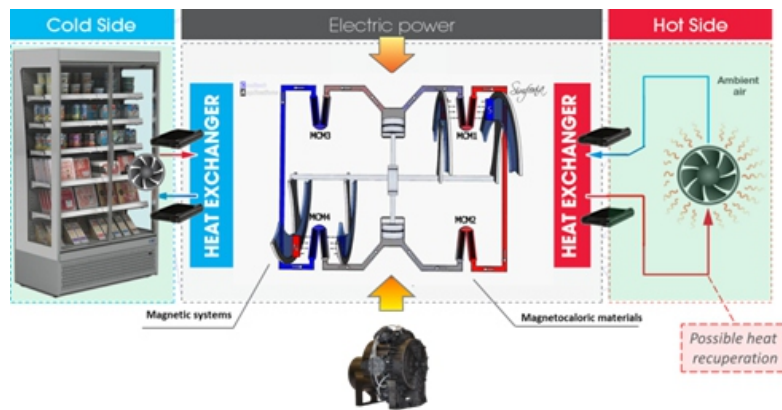


**Fig. 7.** Cooltech Applications' commercial Magnetic Refrigerator Schematic Diagram

## 9 CONCLUSION

The conventional gas compression refrigerators have the primary refrigeration application nowadays, although they are not power-efficient. Refrigerants used in these refrigerators are detrimental for the environment as laid down in the Montreal Protocol. Magnetic Refrigeration is a promising viable alternative for conventional refrigeration. Over the last decade or so, magnetic refrigeration at room temperature has become the subject of considerable attention. This technology makes use of magnetocaloric effect: that is the response of a magnetic solid to an applied magnetic field causing a change in its temperature. RTME provides the advantage of better efficiency (20 – 30%), lesser energy consumption (~50%), absence of any harmful gases, low pressure operation and lower noise generation. A number of prototypes were generated during the era from 1976 to 2016 for room temperature magnetic refrigeration as discussed in the paper. Most of the prototypes had one or more limitations which prevented its industrialization and commercialization. Many companies and institutions around the world came up with different models with different performance parameters. It was not until 2015 that a product by Cooltech applications was launched after years of research. The product can be integrated with conventional refrigerators of comparable capacity. This product has opened the door for further improvement in the RTMR technology for their application in larger capacity refrigerators and air conditioners.

## 10 REFERENCES

- [1] Warburg E. *Magnetische Untersuchungen. I. Ueber einige Wirkungen der Coercitivkraft.* Ann Phys 1881;13:141–64.
- [2] Debye P. *Einige Bemerkungen zur Magnetisierung bei tiefer temperatur.* Ann Phys 1926;81:1154–60.
- [3] Giauque WF. *A thermodynamic treatment of certain magnetic effects. A proposed method of producing temperatures considerably below 1 absolute.* J Amer Chem Soc 1927;49:1864–70.
- [4] Pecharsky VK, Gschneidner Jr KA. *Magnetocaloric effect from indirect measurements: magnetization and heat capacity.* J Appl Phys 1999;86(1):565–75.
- [5] Pecharsky VK, Gschneidner Jr KA. *Some common misconception concerning magnetic refrigerant materials.* J Appl Phys 2001;90(9):4614–22

- [6] H. Osterreicher, F. T. Parker Magnetic cooling near Curie Temperature above 300 K, (1984), *J. Appl. Phys.*, 55, 4334
- [7] Foldeaki, M. schnelle, W. Gmelin, E. Benard, P. Koszegi, B. Giguere, A. Chahine, R. Bose, T. K. (1997), *J. Applies Physics*, 82, 309.
- [8] Schneider, Jr., K. A. Pecharsky, V. K. Bruck, E. Duijin, H. G. M. Levin, E. M. (2000), *Phys. Rev. let.*, 85, 4190.
- [9] Bruck, E. Tegus, O. Thanh, D. T. C. Buschow, K. H. J. (2007), *J. Magn. Magn. Mater.*, 310, 2793
- [10] Yucel, A. Elerman, Y. Aksoy, S. (2005), *Proceedings of the first IIF- IIR International Conference on Magnetic Refrigeration on Room Temperature, Montreux, Switzerland.*
- [11] Benford SM, Brown GV. T-S diagram for gadolinium near the Curie temperature. *J Appl Phys* 1981;52(3): 2110–2.
- [12] Ponomarev BK. Apparatus for measuring the magnetocaloric effect in metal specimens in pulsed up to 8 T. *Instrum Exp Tech* 1983;26:659–62.
- [13] Ponomarev BK. Magnetic properties of gadolinium in the region of paraprocess. *J Magn Magn Mater* 1986;61: 129–38.
- [14] Gopal BR, Chahine R, Bose TK. A sample translator type insert for automated magnetocaloric effect measurements *Rev Sci Instrum* 1997;68(4):1818–22.
- [15] Gopal BR, Chahine R, Fo`ldea`ki M, Bose TK. Noncontact thermoacoustic method to measure the magnetocaloric effect. *Rev Sci Instrum* 1995;66(1):232–8.
- [16] Fo`ldeaki M, Schnelle W, Gmelin E, Benard P, Koszegi B, Gigue`re A, Chahine R, Bose TK. Comparison of magnetocaloric properties from magnetic and thermal measurements. *J Appl Phys* 1997;82(1):309–16.
- [17] Nikitin SA, Talalayeva YV. Features of the magnetic behavior and of the magnetocaloric effect in a single crystal of gadolinium. *Sov Phys JETP* 1978;47:105–9.
- [18] Ivanova TI, Levitin RZ, Nikitin SA, Talalayeva YV. Influence of the field dependence of the magnetic anisotropy constants of gadolinium on the magnetocaloric effect near the Curie point. *Phys Met Metallogr* 1981; 51(4):196–9.
- [19] Kuz'min MD, Tishin AM. Magnetocaloric effect part 2: magnetocaloric effect in heavy rare earth metals and their alloys and application to magnetic refrigeration. *Cryogenics* 1993;33(9):868–82.
- [20] Dan'kov SY, Spichkin YI, Tishin AM. Magnetic entropy and phase transitions in Gd, Tb, Dy and Ho. *J Magn Magn Mater* 1996;152:208–12.
- [21] Fo`ldea`ki M, Chahine R, Bose TK. Magnetic measurements: a powerful tool in magnetic refrigerator design. *J Appl Phys* 1995;77(7):3528–37.
- [22] Dan'kov SY, Tishin AM. Experimental device for studying the magnetocaloric effect in pulse magnetic fields. *Rev Sci Instrum* 1997;68(6):2432–7.
- [23] Dan'kov SY, Tishin AM. Magnetic phase transitions and the magnetothermal properties of gadolinium. *Phys Rev B* 1998;57(6):3478–89.
- [24] Tishin AM, Gschneidner Jr KA, Pecharsky VK. Magnetocaloric effect and heat capacity in the phase-transition region. *Phys Rev B* 1999;59(1):503–11.
- [25] Griffel M, Skochdopole RE, Spedding FH. The heat capacity of gadolinium from 15 to 355 K. *Phys Rev* 1954;93(4):657–61.
- [26] Glorieux C, Thoen J, Bednarz G, White MA, Geldart DJW. Photoacoustic investigation of the temperature and magnetic-field dependence of the specific-heat capacity and thermal conductivity near the Curie point of gadolinium. *Phys Rev B* 1995;52(17):12770–8.
- [27] Pecharsky VK, Moorman JO, Gschneidner Jr KA. 3–350 K fast automatic small sample calorimeter. *Rev Sci Instrum* 1997;68(11):4196–207.
- [28] Gschneidner Jr KA, Pecharsky VK. The influence of magnetic field on the thermal properties of solids. *Mater. Sci Eng* 2000;287:301–10.
- [29] Dai W, Shen BG, Li DX, Gao ZX. New magnetic refrigeration materials for temperature range from 165 K to 235 K. *J Alloys Compounds* 2000;311:22–5.
- [30] Canepa F, Cirafici S, Napoletano M, Merlo F. Magnetocaloric properties of Gd<sub>2</sub>Pd<sub>3</sub> and related intermetallic compounds. *IEEE Trans Magn* 2002;38(5):3249–51.
- [31] Niu XJ, Gschneidner Jr KA, Pecharsky AO, Pecharsky VK. Crystallography, magnetic properties and magnetocaloric effect in Gd<sub>4</sub>(Bi<sub>x</sub>Sb<sub>1-x</sub>)<sub>3</sub> alloys. *J Magn Magn Mater* 2001;234:193–206.
- [32] Pecharsky VK, Gschneidner Jr KA. Tunable magnetic regenerator alloys with a giant magnetocaloric effect for magnetic refrigeration from ~20 to ~290 K. *Appl Phys Lett* 1997;70(24):3299–301.

- [33] Pecharsky VK, Gschneidner Jr KA. Effect of alloying on the giant magnetocaloric effect of  $Gd_5(Si_2Ge_2)$ . *J Magn Magn Mater* 1997;167:179–84.
- [34] Pecharsky VK, Gschneidner Jr KA. Giant magnetocaloric effect in  $Gd_5(Si_2Ge_2)$ . *Phys Rev Lett* 1997;78(23): 4494–7.
- [35] Pecharsky VK, Gschneidner Jr KA. Phase relationships and crystallography in the pseudobinary system  $Gd_5Si_4-Gd_5Ge_4$ . *J Alloys Compounds* 1997;260:98–106.
- [36] Pecharsky VK, Gschneidner Jr KA. The giant magnetocaloric effect in  $Gd_5(Si_xGe_{1-x})_4$  materials for magnetic refrigeration. *Adv Cryo Eng* 1998;43:1729–36.
- [37] Morellon L, Algarabel PA, Ibarra MR, Blasco J, Garcí'a-Landa B, Arnold Z, Albertini F. Magnetic-field-induced structural phase transition in  $Gd_5(Si_{1.8}Ge_{2.2})$ . *Phys Rev B* 1998;58(22):R14721–R14724.
- [38] Gigue' re A, Fo' ldea' ki M, Gopal BR, Chahine R, Bose TK. Direct measurement of the 'Giant' adiabatic temperature change in  $Gd_5Si_2Ge_2$ . *Phys Rev Lett* 1999; 83(11):2262–5.
- [39] Gschneidner Jr KA, Pecharsky VK, Pecharsky AO, Ivchenko VV, Levin EM. The nonpareil  $R_5(Si_xGe_{1-x})_4$  phases. *J Alloys Compounds* 2000;303–304:214–22.
- [40] Morellon L, Blasco J, Algarabel PA, Ibarra MR. Nature of the first-order antiferromagnetic-ferromagnetic transition in the Ge-rich magnetocaloric compounds  $Gd_5(Si_xGe_{1-x})_4$ . *Phys Rev B* 2000;62(2):1022–6.
- [41] Levin EM, Gschneidner Jr KA, Pecharsky VK. Magnetic properties of  $Gd_5(Si_{1.5}Ge_{2.5})$  near the temperature and magnetic field induced first order phase transition. *J Magn Magn Mater* 2001;231:235–45.
- [42] Jean Claude Heitzeler, Christian Mülle, US 8769966 B2, Thermal generator using magnetocaloric material, Jul 8, 2014
- [43] Pecharsky AO, Pecharsky VK, Gschneidner Jr KA. Uncovering the structure–property relationships in  $R_5(Si_xGe_{4-x})$  intermetallic phases. *J Alloys Compounds* 2002;344:362–8.
- [44] Zhang XX, Tejada J. Magnetocaloric effect in  $La_{0.67}Ca_{0.33}MnO_3$  and  $La_{0.60}Y_{0.07}Ca_{0.33}MnO_3$  bulk materials. *Appl Phys Lett* 1996;69(23):3596–8.
- [45] Hamilton JJ, Keatley EL, Ju HL, Raychaudhuri AK, Smolyaninova VN, Greene RL. Low temperature specific heat of  $La_{0.6}Ba_{0.33}MnO_3$  and  $La_{0.8}Ca_{0.2}MnO_3$ . *Phy Rev B* 1996;54(21):14926–9.
- [46] Chen W, Zhong W, Hou DL, Du YW. Research on magnetocaloric effect of  $La_{1-x}K_xMnO_3$ . *Journal of Hebei University of Science and Technology* 1998;19(1): 13–16.
- [47] Guo ZB, Du YW, Zhu JS, Huang H, Ding WP, Feng D. Large magnetic entropy change in perovskite-type manganese oxides. *Phys Rev Lett* 1997;78(6):1142–5.
- [48] Bohigas X. Tunable magnetocaloric effect in ceramic perovskites. *Appl Phys Lett* 1998;73(3):390–2.
- [49] ZhongW, ChenW, DingWP, Zhang N, Du YW, Yan QJ. Magnetocaloric properties of Na-substituted perovskite type manganese oxides. *Solid State Commun* 1998;106(1): 55–8.
- [50] Guo ZB, Yang W, Shen YT, Du YW. Magnetic entropy change in  $La_{0.75}Ca_{0.25-x}Sr_xMnO_3$  perovskites. *Solid State Commun* 1998;105(2):89–92.
- [51] Guo ZB, Yang W, Shen YT, Du YW. Large magnetic entropy change in  $La_{0.75}Ca_{0.25}MnO_3$ . *Appl Phys Lett* 1997;70(7):904–5.
- [52] Woodfield BF, Wilson ML, Byers JM. Low-temperature specific heat of  $La_{1-x}Sr_xMnO_{3+d}$ . *Phy Rev Lett* 1997; 78(16):3201–4.
- [53] Gu G, Cai JH, Yang W, Du YW. Magnetotransport and magnetocaloric properties of  $La_{0.55}Er_{0.05}Ca_{0.4}MnO_3$ . *J Appl Phys* 1998;84(7):3798–801.
- [54] Bohigas X, del Barco E, Sales M, Tejada J., Magnetocaloric effect in  $La_{0.65}Ca_{0.35}Ti_{1-x}Mn_xO_3$  ceramic perovskites. *J Magn Magn Mater* 1999;196–197:455–7.
- [55] Bohigas X, Tejada J, Mari'nez-Sarrio' n ML, Tripp S, Black R. Magnetic and calorimetric measurements on the magnetocaloric effect in  $La_{0.6}Ca_{0.4}MnO_3$ . *J Magn Magn Mater* 2000;208:85–92.
- [56] Szweczyk A, Szymczak A, Wis'niewski A, Piotrowski K, Kartaszy' ski R, Da, browski B, Koles'nik S, Bukowski Z. Magnetocaloric effect in  $La_{1-x}Sr_xMnO_3$  for  $x=0.13$  and  $0.16$ . *Appl Phys Lett* 2000;77(7):1026–8.
- [57] Sun Y, Xu XJ, Zhang YH. Large magnetic entropy change in the colossal magnetoresistance material  $La_{2/3}Ca_{1/3}MnO_3$ . *J Magn Magn Mater* 2000;219:183–5.
- [58] Tang T, GuKM, Cao QQ, WangDH, Zhang SY, DuYW. Magnetocaloric properties of Ag-substituted perovskite type manganites. *J Magn Magn Mater* 2000;222:110–4.
- [59] Wang ZM, Ni G, Xu QY, Sang XH, Du YW. Magnetic entropy change in perovskite manganites  $La_{0.65}Nd_{0.05}Ca_{0.3}Mn_{0.9}B_{0.1}O_3$  ( $B=Mn, Cr, Fe$ ). *J Magn Magn Mater* 2001;234:371–4.



- [60] Sun Y, Salamon MB, Chun SH. Magnetocaloric effect and temperature coefficient of resistance of  $\text{La}_{2/3}(\text{Ca,Pb})_{1/3}\text{MnO}_3$ . *J Appl Phys* 2002;92(6):3235–8.
- [61] Osterreicher H, Parker FT. Magnetic cooling near Curie temperature above 300K. *J Appl Phys* 1984;55:4334–8.
- [62] Wang BZ, Cao XM, Wen M. The researching for property of cooling by magnetic cycling about  $\text{Re}_2\text{Fe}_{17}$  type rare earth metal compounds. *Journal of Hebei University of Technology* 2000;29(5):87–91
- [63] Hu FX, Shen BG, Sun JR, Wu GH. Large magnetic entropy change in a Heusler alloy  $\text{Ni}_{52.6}\text{Mn}_{23.1}\text{Ga}_{24.3}$  single crystal. *Phys Rev B* 2001;64(13):132412.
- [64] Hu FX, Shen BG, Sun JR. Magnetic entropy change in  $\text{Ni}_{51.5}\text{Mn}_{22.7}\text{Ga}_{25.8}$  alloy. *Appl Phys Lett* 2000;76(23): 3460–2.
- [65] Wada H, Tanabe Y. Giant magnetocaloric effect of  $\text{MnAs}_{1-x}\text{Sb}_x$ . *Appl Phys Lett* 2001;79(20):3302–4.
- [66] Wada H, Taniguchi K, Tanabe Y. Extremely large magnetic entropy change of  $\text{MnAs}_{1-x}\text{Sb}_x$  near room temperature. *Mater Trans JIM* 2002;43(1):73–7. 634 B.F. Yu et al. / *International Journal of Refrigeration* 26 (2003) 622–636
- [67] Tegus Q, Bruck E, Buschow KHJ, de Boer FR. Transition-metal-based magnetic refrigerants for room-temperature applications. *Nature* 2002;415(10):150–2
- [68] Hashimoto T, Kuzuhara T, Matsumoto K, Sahashi M, Imonata K, Tomokiyo A, Yayama H. A new method of producing the magnetic refrigerant suitable for the Ericsson magnetic refrigeration. *IEEE Trans Magn* 1987; 23(5):2847–9.
- [69] Hashimoto T, Kuzuhara T, Sahashi M, Inomata K, Tomokiyo A, Yayama H. New application of complex magnetic materials to the magnetic refrigerant in an Ericsson magnetic refrigerator. *J Appl Phys* 1987;62(9): 3873–8.
- [70] Smaili A, Chahine R. Composite materials for Ericsson like magnetic refrigeration cycle. *J Appl Phys* 1997;81(2): 824–9..
- [71] Shao YZ, Lai JKL, Shek CH. Preparation of nanocomposite working substances for room-temperature magnetic refrigeration. *J Magn Magn Mater* 1996;163: 103–8.
- [72] Shao YZ, Zhang JX, Lai JKL, Shek CH. Magnetic entropy in nanocomposite binary gadolinium alloys. *J Appl Phys* 1996;80(1):76–80.
- [73] Krill CE, Merzoug F, Krauss W, Birringer R. Magnetic properties of nanocrystalline Gd and W/Gd. *NanoStruc Mater* 1997;9:455–8.
- [74] Shull RD. Magnetocaloric effect of ferromagnetic particles. *IEEE Trans Magn* 1993;29(6):2614–5.
- [75] Shull RD, McMichael RD, Ritter JJ. Magnetic nanocomposites for magnetic refrigeration. *Nanostructured Matter* 1993;2(2):205.
- [76] Chang SN, Yan XG. Thermodynamic norm for selecting refrigerant of magnetic refrigeration near room temperature. *Journal of Beijing University of Aeronautics and Astronautics* 1997;23(5):639–42.
- [77] Cross CR, Barclay JA, Degregoria AJ, Jaeger SR, Johnson JW. Optimal temperature–entropy curves for magnetic refrigeration. *Adv Cryo Eng* 1988;33:767–75.
- [78] Yan ZJ, Chen JC. A note on the Ericsson refrigeration cycle of paramagnetic salt. *J Appl Phys* 1989;66(5):2228–9.
- [79] Yan ZJ, Chen JC. The characteristic of polytropic magnetic refrigeration cycles. *J Appl Phys* 1991;70(4):1911–4.
- [80] Chen JC, Yan ZJ. The effect of field-dependent heat capacity on regeneration in magnetic Ericsson cycles. *J Appl Phys* 1991;69(9):6245–7.
- [81] Yan ZJ, Chen JC. The effect of field-dependent heat capacity on the characteristics of the ferromagnetic Ericsson refrigeration cycle. *J Appl Phys* 1992;72(1):1–5.
- [82] Dai W. Regenerative balance in magnetic Ericsson refrigeration cycles. *J Appl Phys* 1992;71(10):5272–4.
- [83] Lixuan Chen and Zijun Yan, Main characteristics of a Brayton refrigeration cycle of paramagnetic salt, *J. Appl. Phys.* 75, 1249 (1994)
- [84] Yulin Yang, Jincan Chen , Jizhou He, E. Brück, Parametric optimum analysis of an irreversible regenerative magnetic Brayton refrigeration cycle, *PhysicaB: Condensed Matter*, –Volume 364, Issues 14, 15 July 2005, Pages 33–42
- [85] Zhengrong Xia, Yue Zhang, Jincan Chen, Guoxing Lin, Performance analysis and parametric optimal criteria of an irreversible magnetic Brayton-refrigerator, *Applied Energy*, –Volume 85, Issues 23, February–March 2008, Pages 159–170

- [86] Bezaguet A, Casas-Cubillos J, Cyvoct A, Lebrun Ph, Losserand-Madoux R, Marquet M, Schmidt M. A pulsed superconducting magnet for a static magnetic refrigerator operating between 1.8K and 4.5K. *IEEE Trans Magn* 1994;30(4):2138–41.
- [87] Rowe JR, Hertel JA, Barclay JA, Cross CR, Trueblood JR, Hill DD. Conductively cooled Nb<sub>3</sub>Sn magnet system for a magnetic refrigerator. *IEEE Trans Magn* 1991; 27(2):2377–80.
- [88] Trueblood JR, Claybaker PJ, Johnson JW, Stankey TM. A vertically reciprocating NbTi solenoid used in a regenerative magnetic refrigerator. *IEEE Trans Magn* 1991;27(2):2384–6
- [89] Lebouc, A., Allab, F., Fournier, J.M., Yonnet, J.P. (2005). Réfrigération magnétique, [RE 28], *Techniques de l'Ingénieurs*.
- [90] Engelbrecht, K.L., Nellis, G.F., Klein, S.A., Boeder, A.M. (2005). Modeling Active Magnetic Regenerative Refrigeration Systems, *International Conference on Magnetic Refrigeration at Room Temperature*, Montreux, Switzerland.
- [91] Tura, A., Rowe, A. (2007). Design and testing of a permanent magnet magnetic refrigerator. *Proceedings of the Second International Conference on Magnetic Refrigeration at Room Temperature*, Portoroz, Slovenia, 11-13 April. *International Institute of Refrigeration, Paris*, pp. 363-371.
- [92] Yu, B.F., Gao, Q., Zhang, B., Meng, X.Z., Chen, Z., 2003. Review on research of room temperature magnetic refrigeration. *International. Journal of Refrigeration*. 26, 622- 636.
- [93] Matsumoto K, Hashimoto T. Thermodynamic analysis of magnetically active regenerator from 30 to 70 K with a Brayton-like cycle. *Cryogenics* 1990;30:840–5
- [94] Degregoria AJ. Modeling the active magnetic regenerator. *Adv Cryo Eng* 1992;37B:867–73.
- [95] Reid CE, Barclay JA, Hall JL, Sarangi S. Selection of magnetic materials for an active magnetic regenerative refrigerator. *J Alloys Compounds* 1994;207/208:366–71.
- [96] Pecharsky VK, Gschneidner Jr KA. Magnetocaloric effect and magnetic refrigeration. *J Magn Magn Mater* 1999;200:44–56.
- [97] Bjork, R., Bahl, C.R.H., Smith, A., Pryds, N. (2010). Review and comparison of magnet designs for magnetic refrigeration. *International. Journal of Refrigeration*. 33, 437-448.
- [98] Brown GV. Magnetic heat pumping near room temperature. *J Appl Phys* 1976;47(8):3673–80.
- [99] Steyert WA. Stirling-cycle rotating magnetic refrigerators and heat engines for use near room temperature. *J Appl Phys* 1978;49(3):1216–26.
- [100] Barclay JA, Steyert WA. Active magnetic regenerator. US Patent No. 4,332,135, 1 June, 1982.
- [101] Zimm C, Jastrab A, Sternberg A, Pecharsky VK, Gschneidner Jr KA, Osborne M, Anderson I. Description and performance of a near-room temperature magnetic refrigerator. *Adv Cryog Eng* 1998;43:1759–66.
- [102] Vasile, C., Müller, C., 2005. A new system for a magnetocaloric refrigerator. In: Egolf, P.W., et al. (Eds.), *Proceedings of First International Conference on Magnetic Refrigeration at Room Temperature*, Montreux, Switzerland, 27e30 September. *International Institute of Refrigeration, Paris*, pp. 357e366.
- [103] Vasile, C., Müller, C., 2006. Innovative design of a magnetocaloric system. *International Journal of Refrigeration* 29 (8), 1318e1326.
- [104] Müller, C., Bour, L., Vasile, C., 2007. Study of the efficiency of a magnetothermal system according to the permeability of the magnetocaloric material around its Curie temperature. In: *Proceedings of the Second International Conference on Magnetic Refrigeration at Room Temperature*, Portoroz, Slovenia, 11e13 April. *International Institute of Refrigeration, Paris*, pp. 323e330.
- [105] Jean Claude Heitzeler, Christian Muller, US 8869541 B2, Thermal generator with magnetocaloric material and incorporated heat transfer fluid circulation means, Oct 28, 2014
- [106] Jean Claude Heitzeler, Christian Muller, US 8978391 B2, Method for generating a thermal flow and magnetocaloric thermal generator, Mar 17 2015
- [107] Bingfeng Yu, Min Liu, Peter W. Egolf, Andrej Kitanovski, A review of magnetic refrigerator and heat pump prototypes built before the year 2010, *International Journal of Refrigeration*, 33 (2010), 1029 – 1060
- [108] Housseem Rafik El-Hana Bouchekara and Mouaaz Nahas, Department of Electrical Engineering, College of Engineering and Islamic Architecture, Umm Al-Qura University, Makkah, *Magnetic Refrigeration Technology at Room Temperature, Trends in Electromagnetism – From Fundamentals to Applications*
- [109] Thesis by Jyotish Chandra Debnath, *Novel Magnetocaloric materials and room temperature magnetic refrigeration*, University of Wollongong, (2011)
- [110] Prakash Chawla, Ankit Mathur, A Review Paper on Development of Magnetic Refrigerator at Room Temperature, (*IJRSE*) *International Journal of Innovative Research in Science & Engineering*, Vol 3, Iss. 3, 2347-3207,

# Development of Risk Based Maintenance Strategy For Gas Turbine Power System

Asis Sarkar\*, D.K. Behera\*\*

\*Department of Mechanical Engineering, National Institute of Technology, Agartala, India

\*\*IGIT, Odissa

## **ABSTRACT**

*The unexpected failures, the down time associated with such failures, the loss of production and, the higher maintenance costs are major problems in any power plant. Risk- based maintenance (RBM) approach helps in designing an alternative strategy to minimize the risk resulting from breakdowns or failures. The RBM methodology is comprised of four modules: viz - identification of the scope, risk assessment, risk evaluation, and maintenance planning. Using this methodology, one is able to estimate risk caused by the unexpected failure as a function of the failure probability and the consequences of failure. Critical equipment can be identified based on pre-selected acceptable level of risk. Maintenance of equipment is prioritized based on the risk, which helps in reducing the overall risk of the plant. The case study of a power-generating unit in the Rukhia gas turbine power plant system is used to illustrate the methodology. Results indicate that the methodology is successful in identifying the critical equipment and in reducing the risk of failure of the equipment. Risk reduction is achieved through the adoption of a maintenance plan which not only increases the reliability of the equipment but also reduces the cost of maintenance including the cost of failure.*

**Keywords:** Maintenance, Risk based maintenance, failure, preventive maintenance, operation.

## **1. INTRODUCTION**

The systems can undergo failures. The failures cause disastrous consequences in human life. The occurrence of failures in manufacturing systems devoted to the production of goods has not so devastating effects but causes, in general, economic losses due to the downtime and the lack of system availability. But in case of process industry the cause of failures are serious. In the case of Gas turbine plant the shut down of critical components will cause serious effect to the loss of human beings and loss of revenue due to shutdown.

Maintenance is crucial to manufacturing operations. In many times the facilities and the production equipment represent the majority of invested capital and deterioration of these facilities and equipment increases production cost and reduce production quality. Managers schedule PM actions to prevent breakdown and equipment deterioration. However to maximize return on their equipment investment

manager attempt to identify the risky equipments required time interval between P.M. actions which will balance the costs of P.M. and the cost of breakdowns and equipment deterioration. When possible managers use the equipment's history card to schedule sets of maintenance tasks together. For example managers can minimize down time by scheduling a set of PM actions during the same period and if possible during machine setup. In practice scheduling maintenance activities always involve some risk. Even those firms which know the failure distribution of components still have some probability of component failure before the scheduled PM action.

The Risk based maintenance system identifies the critical equipment on the basis of risk evaluation. An overall equipment and component maintenance plan is carried out to reduce the risk of operation. By pre scheduling the maintenance activities in improved RBM approaches the consequences of failures and down time can be reduced to minimum level for which the criteria considered are set up financial risks and are presented in this paper. An extensive joint probability density function (PDF) of successive failures and the final survival is proposed to estimate the parameters of the failure distribution and maintenance effect. Economic risk criteria are proposed on the basis of maintenance expenditure. A periodic and imperfect PM plan for equipment in high-risk subsystems is established to meet the risk criteria.

## **2. LITERATURE REVIEW**

There has been an increased focus on risk-based maintenance optimization in the offshore industry prompted by the recent functional regulations on risk. Ape land and Aven (1999) presented alternative probabilistic frameworks for this optimization using a Bayesian approach [1]. The American Society of Mechanical Engineers (ASME) recognized the need of risk-based methods and organized a number of multi disciplinary research task forces to study risk-based in-service inspection and testing. A series of ASME publications present this work, which includes both nuclear and industrial applications (ASME,1991).[2].Backlund and Hannu (2002) discussed maintenance decisions based on risk analysis results. An effective use of resources can be achieved by using risk-based maintenance decisions to determine where and when to perform maintenance and proved the need of homogenized quantitative risk analysis [3]

Balkey and Art (1998) developed a methodology, which includes risk-based ranking methods, beginning with the use of plant PRA (Pre Risk Analysis), for the determination of risk-significant and less risk-significant components for inspection and the determination of similar populations for pumps and valves in-service testing. This methodology integrates non-destructive examination data, structural reliability risk assessment results, PRA results, failure data and expert opinions [4]

Dey (2001) presented a risk-based model for inspection and maintenance of a cross-country petroleum pipeline that reduces the amount of time spent on inspection. This model does not only reduce the cost of the pipeline maintenance; but also suggests efficient design and operational philosophies, construction methodology, and logical insurance plans. The risk-based model uses an analytical hierarchy process and a multiple attribute decision-making technique to identify the factors that influence the failure of a specific pipeline segment. This method could be used to prioritize the inspection and maintenance of pipeline segments. [5]

Industries worldwide spend a huge amount of money on maintenance of production machinery. Each year US industry spends well over \$300 billion on plant maintenance and operation (Dhillon, 2002). [6] Furthermore, it is estimated that approximately 80% of the industry dollars are spent to address chronic failures of the equipment and injury to people. An operating cost reduction of about 40–60% can be achieved through effective maintenance strategies (Dhillon, 2002) [6]. Dadson developed a failure model based on the Weibull probability distribution which established the optimum interval between PM actions as a function of the Weibull scale parameter ( $\theta$ ). [7]. Hagemeijer and Kerkveld (1998) developed a methodology for risk-based inspection of pressurized systems. The methodology is based on the determination of risk by evaluating the consequences and the likelihood of equipment failure. Likelihood of equipment failure is assessed, by means of extrapolation, at the future planned maintenance campaign to identify the necessary corrective work. The study aimed to optimize the inspection and maintenance efforts and to minimize the risk in a petroleum plant in Brunei. [8] Harnly (1998) developed a risk ranked inspection recommendation procedure that is used in one of Exxon's chemical plants to prioritize repairs that have been identified during equipment inspection. The equipment are prioritized based on the severity index, which is failure potential combined with consequences of failure. The reduction in the overall risk of the plant is accomplished by working high risk items first. Making decisions concerning a selection of a maintenance strategy using a risk-based approach is essential to develop cost effective maintenance policies for mechanized and automated systems because in this approach the technical features (such as reliability and maintainability characteristics) are analyzed considering economic and safety consequences [9]

Studies by Khan and Abbasi (1998), views the major challenge for a maintenance engineer is to implement a maintenance strategy, which maximizes availability and efficiency of the equipment; controls the rate of equipment deterioration; ensures a safe and environmentally friendly operation; and minimizes the total cost of the operation. This can only be achieved by adopting a structured approach to the study of equipment [10, 11]. Recently, Khan and Haddara (2003) proposed a new and comprehensive methodology for risk-based inspection and maintenance. The application of



methodology was illustrated using a particular system as a case study. The methodology integrates quantitative risk assessment and evaluation with proven reliability analysis techniques. The equipment is prioritized based on total risk (economic, safety and environmental). A maintenance plan to reduce unacceptable risk is developed [12]

The methodology was also applied to an ethylene oxide production plant (Khan and Haddara, 2004). Dey (2001) presented a risk-based model for inspection and maintenance of a cross-country petroleum pipeline that reduces the amount of time spent on inspection. This model does not only reduce the cost of the pipeline maintenance; but also suggests efficient design and operational philosophies, construction methodology, and logical insurance plans [13]. Kletz (1994), and Kumar (1998) show a strong relationship between maintenance practices and the occurrence of major accidents. Profitability is closely related to the availability and reliability of the equipment [14]. (Kumar, 1998). provides a holistic view of the various decision scenarios concerning the selection of a maintenance strategy where cost consequences of every possible solution can be assessed quantitatively. Risk-based maintenance strategies can also be used to improve the existing maintenance policies through optimal decision procedures in different phases of the risk cycle of a system. Unexpected failures usually have adverse effects on the environment and may result in major accidents [15]. Misewicz, Smith, Nessim, and Playdon (2002) developed a risk-based integrity project ranking approach for natural gas and CO<sub>2</sub> pipelines. The approach is based on a benefit cost ratio, defined as the expected risk reduction in dollars per mile over the project useful life, divided by the total project cost. Risk reduction is estimated using a quantitative risk analysis approach. The benefit cost ratio results can be used as a tool to justify the maintenance budget. [16]. A holistic, risk-based approach to asset integrity management was discussed by Montgomery and Serratela (2002). It is based on proven risk assessment and reliability analysis methodologies, as well as the need to have appropriate management systems. Combining risk assessment and risk-based decision-making tools provides operators with a realistic way to achieve corporate and regulators objectives. The review of the literature indicates that there is a trend to use risk as a criterion to plan maintenance tasks. However, most of the previous studies focused on a particular system and were either quantitative or semi quantitative. [17]

Murty and Naikan suggest a complicated method for designing condition monitoring measurement intervals for all types of machines by considering interval availability, economic factors and four different stages of machine life. A different method of determining the measurement interval is utilized in each of the four different stages. The method is based on the limiting value of the ratio of the repair rate and failure rate, They suggest that much of the information can be obtained from Data collection in

the first year of machine life [18]. **Shore** improved the failure model based on the Weibull probability distribution model with a solution method that required only partial distribution information. However neither Research considered the inherent probability of the early breakdowns. Many of the existing models are difficult to use [19]. Vesely, Belhadj, and Rezos (1993) used probabilistic risk assessment (PRA) as a tool for maintenance prioritization.. The minimal cutset contribution and the risk reduction importance are the two measures that were calculated. Using minimal cutsets and the risk reduction importance, the basic events and their associated maintenance were prioritized. Moreover, basic events having low risk and unimportant maintenances were ignored [20]. Krishnasamy L *et al* developed a risk based maintenance strategy for power generating plant. They presented a case study in which they carried out risk assessment, risk evaluation and developed fault tree to identify the high risk component. Finally they suggested the maintenance procedure for the risky components [21]. The contributions by others in maintenance field are as follows:- Least-cost strategies for asset management (operation, maintenance and capital expenditures) are essential for increasing the revenues of power- generating plants. The risk-centered approach as used in this study helps in making decisions regarding the prioritization of the equipment for maintenance and in determining an appropriate maintenance interval. The present work describes the application of a risk- based maintenance policy for developing a maintenance plan for a gas turbine plant in Rukhia of India.

### 3. RISK BASED MAINTENANCE

#### Methodology

Risk-based maintenance methodology provides a tool for maintenance planning and decision-making to reduce the probability of failure of equipment and the consequences of failure. The resulting maintenance program maximizes the reliability of the equipment and minimizes the cost of the total maintenance cost. Figure. 2 shows a flow diagram , which depicts the process used to develop this methodology. The following steps are followed.

#### 3.1. Identification of the scope:

The plant is divided into major systems, each system is divided into subsystems and the components of each subsystem are identified. Each system is analyzed one at a time, until the whole plant has been investigated. Data required to analyze the potential failure scenarios for each system are collected. Physical, operational, and logical. Relationships between the components are studied. Figure 1 describes the Block Diagram of Single Shaft Gas Turbine Power Plant

### 3.2. Risk assessment

Risk assessment starts with the identification of major potential hazards (top events) that each failure scenario may lead to. A fault tree is used to identify the basic events and the intermediate paths that will lead to the top event. Failure data for the basic events of the subsystem are used to estimate the probability of subsystem failure consequence analysis is used to quantify the effect of the occurrence of each failure scenario. This is based on a study of maintenance costs including costs incurred as a result of failure. Finally, a quantitative measure for risk is obtained.

### 3.3. Risk evaluation:

An acceptable risk criterion is determined and used to decide whether the estimated risk of each failure scenario is acceptable or not. Failure scenarios that produce unacceptable risk are used to determine maintenance policies for the components involved.

### 3.4. Maintenance planning:

Subsystems that failed to meet the acceptable risk criteria are studied with the objective to designing maintenance program that will reduce the risk. Both the type of maintenance and the maintenance interval should be decided upon at this stage. In this work, we only use the maintenance interval to modify the risk. By modifying the maintenance interval, the probability of failure changes and this will also affect the risk involved. The probability of the top event is decided upon using the acceptable risk criterion. A reverse fault tree analysis is used to estimate the new probability of failure for each basic event. Maintenance intervals which produce the new probability of failure are then calculated. However, one can also look at how maintenance is done with a view to reduce the consequence of failure as well.

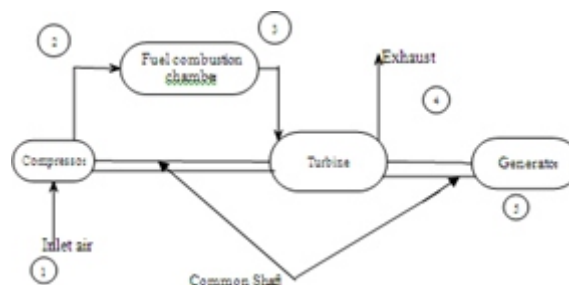


**Figure 1.** Block Diagram of Single Shaft Gas Turbine Power Plant

#### 4. CASE STUDY: GAS TURBINE POWER PLANT

A case study is used to illustrate the use of the above mentioned methodology in designing maintenance programs. The case study uses a power-generating unit in an operating steam power plant. A gas turbine power plant is a means for converting the potential chemical energy of fuel into electrical energy. In its simplest form, it consists of a compressor, combustion chamber and two turbine driving an electrical generator. The gas turbine plant is shown in figure 1.

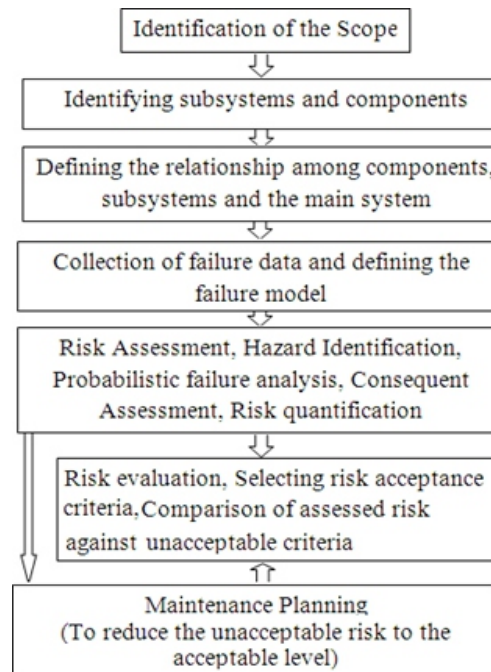


**Figure 2.** Architecture of R.B.M. Methodology

The Rukhia Gas Turbine power plant started operating in 1989 using five units , sixth, seventh and eighth units are added in 1999. The data used in this work was obtained from the Rukhia Gas Turbine power plant in Rukhia around 25 kilometers from Agartala. The unit under study is designated here as Unit 4.

#### 5. CONSEQUENCE ANALYSIS

Consequence analysis involves the estimation of maintenance and the production loss cost. The maintenance cost is calculated using the following equation:  $MC = C_f + DT.C_v$  where  $C_f$  is the fixed cost of failure (cost of spare parts),  $DT$  is the down time, and  $C_v$  is the variable cost per hour of down time, it includes labor rate and crew size. The cost of spares includes the cost of raw material, internally

manufactured parts, the parts sent away for repairs, new spare parts, consumables, small tools, testing equipments, and rent for special equipments. The cost of spares and raw materials is drawn from the plant stock book. For small tools, Rs3.00 is added per man-hour. Special equipments rent cost is derived from plant records. Maintenance down time includes the total amount of time the plant would be out of service as a result of failure, from the moment it fails until the moment it is fully operational again. The repair process itself can be decomposed into a number of different subtasks and delay times as shown in **Figure 3**.

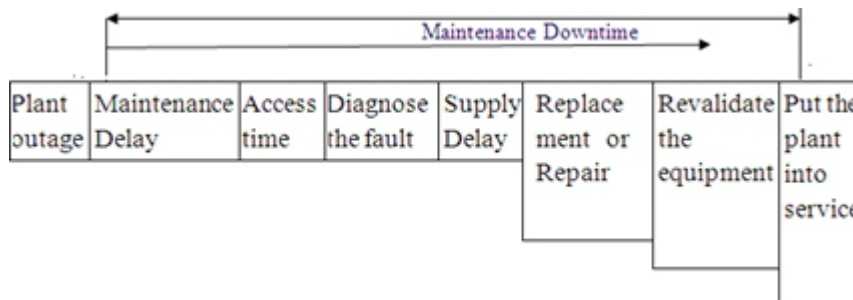


Figure 3 : Analysis of Downtime

**5.1 Estimation of Production loss cost :** The production loss cost is estimated using the following formula  $PLC = DT \cdot PL \cdot SP$ , Where  $DT$  = downtime,  $PL$  = production loss in Megawatt (1 Megawatt =  $10^6$  watt, one watt is the rate at which work is done when one ampere (A) of current flows through an electrical potential difference of one volt (V) and in terms of classical mechanics, one watt is the rate at which work is done when an object's velocity is held constant at one meter per second against constant opposing force of one newton)  $SP$  is the selling price of generated electricity. The cost of labor is an important component of the maintenance cost. This is based on the hourly rate for various trades and the information is drawn from the plant documentation (Table 1 represents the rates used in the present study). Down time associated with forced outage and forced de-rating state is estimated from the failure data collected for the GTPPS. Owing to the lack of data, the down time and the number of maintenance personnel involved in repair is estimated by interviewing the maintenance personnel.

**5.2 Estimation of Probability of failure :** Down time associated with forced outage and forced de-rating state is estimated from the failure data collected for the GTPPS. Owing to the lack of data, the down time and the number of maintenance personnel involved in repair is estimated by interviewing the maintenance personnel. The probability of failure of different components and subcomponents are given in table 2,3,4,5,6,7 respectively collecting from the plant Data. Production loss in Mega Watt hour was computed from the failure data. A price for fuel was estimated at Rs 45.00 per cubic centimeter. The price was derived from the cost of the Gases collected from GAIL. This price includes overheads, the combination of production loss cost and the maintenance cost gives the consequence of the failure in Rupees. Risk is calculated using the results of the previous two steps, by multiplying the probability and the consequence of failure.

**Table 1.** Labor Rates of Different categories

Trade	Description	Hourly Rate
Boiler maker \$	General foreman	Rs 46.21/-
	Foreman	44.90
	Fitter/welder	41.26/-
	Apprentice 3	38.04
	Apprentice 2	32.81
	Apprentice 1	27.64
	Helper	38.04
Pipe fitter	Foreman	45.49
	Welder/journeyman	42.64
Mill wright	Foreman	41.47
	Welder/journeyman	40.22
	Apprentice	38.60
	Journey	34.64
	Electrician	25.00

**Table 2.** Summary values of failures in Generator

Component	Name of the Problem	Total failure observed	Total repair time taken	$\lambda$ value
P.m.g. bolt	P.m.g. bolt broken	6	6	$6.1896 \times 10^{-04}$
P.m.g. bush	P.m.g. bush changed	40	44	$4.1264 \times 10^{-03}$
P.m.g. shaft	Bush not in alignment of the generator	4	20	$4.1264 \times 10^{-04}$
Component	Name of the Problem	Reliability = $e^{-\lambda t}$ T= 12000	Probability of failure $1 - e^{-\lambda t}$	Failure probability of the system
P.m.g. bolt	P.m.g. bolt broken	0.000593	0.999407	0.9974
P.m.g. bush	P.m.g. bush changed	0.000318	1	
P.m.g. shaft	Bush not in alignment of the generator	0.00708	0.9928	

**Risk evaluation:** An acceptable risk criterion was determined based on the yearly maintenance expenditure of Unit 4. (found from records as Rs 2,000,000 per year) The estimated risk for each individual subsystem was compared against the acceptable risk criterion. Subsystems whose estimated risk exceeded the acceptance criteria were identified. These are the units whose maintenance plan had



to be modified in order to lower their risk. To facilitate this comparison, a risk index was calculated. The risk index is the actual risk divided by the acceptable risk. The risk indexes and probability of failures and consequences of different components are described in table 8 and 9.

**Table 3.** Summary value of failures of other systems (electrical system)

Component	Name of the Problem	Total failure observed	Total repair time taken	$\lambda$ value
Generator breaker	Desynchronization	33	62	$0.3125 \times 10^{-03}$
Relay	Relay fault	8	16	$0.1875 \times 10^{-03}$
Control system	Under frequency	11	14	$0.125 \times 10^{-03}$
Feeder	Synchronization	10	26	$0.375 \times 10^{-03}$
Bus bar	Feeder fault	9	10	$0.4783 \times 10^{-03}$
Gas collecting tank	Poor demand & shortage of Gas	11	39	$0.125 \times 10^{-03}$
Grid	Grid failure	12	14	$0.1340 \times 10^{-03}$

Component	Reliability = $e^{-\lambda t}$ T= 20000	Probability of failure 1- $e^{-\lambda t}$	Failure probability of the system
Generator breaker	0.00193	0.99807	0.9678
Relay	0.0235	0.9765	
Control system	0.0626	0.9374	
Feeder	0.005531	0.994469	
Bus bar	0.00007	0.9993	
Gas collecting tank	0.0626	0.9374	
Grid	0.0685	0.9315	

**Table 4.** Summary values of failures of compressor systems

Component	Name of the Problem	Total failure observed	Total repair time taken	$\lambda$ value
Turbine housing	Exhaust over temperature	5	11	$1.6675 \times 10^{-03}$
Servo valve	Servo trouble	3	8	$1.005 \times 10^{-03}$
bearing	Oil leakage	2	7	$0.667 \times 10^{-03}$
Air filter module	Turbine air inlet differential high	6	18	$2.001 \times 10^{-03}$

Component	Reliability = $e^{-\lambda t}$ T=10000	Probability of failure $1 - e^{-\lambda t}$	Failure probability of the system
Turbine housing	0.0000057	1	0.9996
Servo valve	0.0000045	1	
bearing	0.001265	0.99871	
Air filter module	0.0000002	0.99998	

## 6. MAINTENANCE PLANNING

The strategy that was adopted to lower the risk to meet the acceptable criterion, was to reduce the probability of failure. Based on the evaluation results the components are segregated into three types. High Risk items are high pressure turbine and combustion chamber and medium risk items are Permanent magnet generator bush (pmg), Servo valve, Turbine housing, Air filter module, and generator breaker. The rest 25 components are low Risk equipment. The high risk main equipments (Risk value more than 1.0) are high pressure turbine, compressor and combustion chamber and medium risk items are other electrical system and generator. The rest equipments are in Low class category. As a thumb rule without going to the complex equation The maintenance intervals are set as per the following Criteria ::

High risk items -----3 months

Medium risk items -----6 months

and Low risk items are 1 year

**Table 5.** Summary values of failures of combustion systems

Component	Name of the Problem	Total failure observed	Total repair time taken	$\lambda$ value
Combustion chamber	Loss of flame	48	79	$3.928 \times 10^{-03}$
Servo valve	Servo valve problem	4	4	$0.327 \times 10^{-03}$
2 <sup>nd</sup> stage Nozzle	Nozzle Problem	4	21	$0.327 \times 10^{-03}$
Bearing 2	Bearing drain temperature high	2	3	$0.164 \times 10^{-03}$
starter	Starting and electrical problem	5	7	$0.4092 \times 10^{-03}$



Component	Reliability $= e^{-\lambda t}$ $T = 10000$	Probability of failure $1 - e^{-\lambda t}$	Failure probability of the system
Combustion chamber	0.0000002	1.0	0.943
Servo valve	0.38996	0.9619935	
2 <sup>nd</sup> stage Nozzle	0.38996	0.9619935	
Bearing 2	0.19398	0.80602	
starter	0.0167	0.98329	

The modified maintenance interval of main equipments for compensating risk parameters are described. Similarly the maintenance interval of sub components are also prepared for the components (subsystem of equipments) and are as follows::

High risk items -----2 months

Medium risk items -----5 months

and Low risk items are-----10 months

The modified maintenance interval of sub components for compensating risk parameters are described.

**Table 7.** Summary values of failures of L.P. Turbine system

Component	Name of the Problem	Total failure observed	Total repair time taken	$\lambda$ value
L.P. turbine	L. P. over speed	6	15	$0.1265 \times 10^{-03}$
2 <sup>nd</sup> stage nozzle	Nozzle problem	1	1	$0.021 \times 10^{-03}$
Diesel engine	Start up problem	2	7	$0.021 \times 10^{-03}$
Bearing header	Lub oil header temp high	2	9	$0.04217 \times 10^{-03}$
Bearing 2 and 4	Oil leakage	1	2	$0.021 \times 10^{-03}$

**Table 6.** Summary values of failures of H.P Turbine system

Component	Name of the Problem	Total failure observed	Total repair time taken	$\lambda$ value
HP turbine	H. P turbine under speed	21	30	$0.442 \times 10^{-03}$
Mist eliminator	Heavy smoke	2	2	$0.04217 \times 10^{-03}$
	Turbine under speed/locked	1	2	$0.021 \times 10^{-03}$
Lp turbine	Servo problem	1	1	$0.021 \times 10^{-03}$
Servo valve	Exhaust over temp	2	3	$0.04217 \times 10^{-03}$
Turbine housing	Low Hydraulic Pressure	2	4	$0.04217 \times 10^{-03}$
Auxiliary hydraulic pump	Lub oil level low	2	4	$0.04217 \times 10^{-03}$
Lub oil sump	Lub oil drain temp High	2	9	$0.04217 \times 10^{-03}$

Component	Reliability $= e^{-\lambda t}$ T= 10000	Probability of failure $1 - e^{-\lambda t}$	Failure probability of the system
HP turbine	0.012034	0.987965	0.795
Mist eliminator	0.0012034	0.99879	
	0.81058	0.18942	
Lp turbine	0.81058	0.18942	
Servo valve	0.0012034	0.99879	
Turbine housing	0.0012034	0.99879	
Auxiliary hydraulic pump	0.0012034	0.99879	
Lub oil sump	0.0012034	0.99879	

Component	Reliability $y = e^{-\lambda t}$ T= 10000	Probability of failure $1 - e^{-\lambda t}$	Failure probability of the system
L.P. turbine	0.0000032	0.9999967	0.51340
2 <sup>nd</sup> stage nozzle	0.81058	0.18942	
Diesel engine	0.81058	0.18942	
Bearing header	0.0012034	0.99879	
Bearing and 4	0.81058	0.18942	

**Table 8.** calculation of Probability of failures and consequences

Rank	Major system	Consequence in millions	Probability of failure over 20 years
1	Combustion chamber	3,678,481	0.943
2	H.P Turbine	2,478,842	0.795
3	Compressor	2,102,023	0.9996
4	Other electrical system	1,634,060	0.9974
5	Generator	11,110,57	0.9974
6	L.P. Turbine	874,745	0.51340

**Table 9.** calculation of Risk index

Rank	Major system	Risk (\$) over 20 years	Risk index considering accepted risk=2000000
1	Combustion chamber	3468807	1.734
2	H.P Turbine	1970679	1.25786
3	Compressor	2093615	1.046
4	Other electrical system	1629811	0.815
5	Generator	1110768	0.5554
6	L.P. Turbine	449094	0.22455

## 7. RESULT

Risk assessment results are given in Table 8. Any subsystem whose risk index is greater than 1.0 is considered (see Table 8). Three subsystems were found to violate the risk criterion: the Combustion chamber, H.P Turbine, and the Compressor. A new maintenance schedule had to be developed for these three subsystems. To find out which components contribute more the high-risk levels of these subsystems, a study of the components of the subsystems was carried out.. The components were divided in three categories, high risk (risk index value greater than 0.6), medium risk (risk index value between 0.2 and 0.6), and low risk (risk index value less than 0.2).

## 8. SUMMARY AND CONCLUSION

The paper presents a methodology for designing maintenance programs based on reducing the risk of failure. This approach ensures that not only the reliability of equipment is increased but also that the cost of maintenance including the cost of failure is reduced. This will contribute to the availability of the plant as well as its safe operation. In the present approach, only the maintenance interval was considered. This affects the probability of failure directly, but its effect on the consequence of risk is indirect. In deciding the maintenance interval, we grouped the equipment that would be maintained at

the same time together and assigned the minimum length of the maintenance interval for the whole group. This means that some equipment will be over maintained. However, the resulting savings in terms of reducing the down time required to perform the maintenance tasks justify this policy. The study identified the critical equipment based on risk. For example, three Components were found to have unacceptable initial risks. These are the combustion chamber, compressor, high pressure turbine. Reducing the individual risk of each of these components will result in an overall reduction in the risk of the unit. A study of the risk patterns of the components showed that 6% of the items are high risk items.. and 16% of the items followed medium risk items. The remaining 79% of the component are low risk components.

## 9. FUTURE SCOPE FOR RESEARCH

- (1) The reliability of the component can be improved further if maintenance intervals are estimated mathematically, So scopes for further improvement lies in this topic.
- (2) The fault tree analysis can be incorporated for further reducing the risk.
- (3) The possibility of incorporating online monitoring system can be incorporated.
- (4) Effect of maintenance on failures can be studied specially on high risk equipments
- (5) A cost benefit analysis can be done for high and medium risk equipment.

## REFERENCES

- [1] J J Apeland, S., and Aven, T. (1999) "Risk based maintenance optimization: Foundational issues", *Reliability Engineering and System Safety*, 67, 285–292.
- [2] RB] ASME., (1991), "Risk based inspection development guidelines", CRTD 20-1. Washington, DC: American Society of Mechanical Engineers.
- [3] JJ Backland F and Hannu J. (2002) "Can we make maintenance decisions on risk analysis results?" , *Journal of Quality in Maintenance Engineering*, 8(1), 77–91.
- [4] JJ Balkey, R. K., and Art, J. R. (1998), "ASME risk-based in service inspection and testing: An outlook to the future". *Society for Risk Analysis*, 18(4)..
- [5] J J Dey P. M. (2001) "A risk-based model for inspection and maintenance of cross-country petroleum pipeline". *Journal of Quality in Maintenance Engineering*, 40(4), 24–31.
- [6] B] Dhillon, B. S., (2002) , "Engineering maintenance, a modern approach". New York: CRC Press. .
- [7] JJ Dodson, B.,(1994), "Determining the Optimum schedule for Preventive maintenance", *Quality Engineering*, volume 6, pp 667-79.
- [8] TJ Hagemeijer, P. M., & Kerkveld, G. (1998) "A methodology for risk base inspection of pressurized systems." *Selected topics on aging management, reliability, safety and license renewal*, ASME, PVP, (Vol. 444).
- [9] JJ Harnly, A. J. (1998), "Risk based prioritization of maintenance repair work". *Process Safety Progress*, 17(1), 32–38.
- [10] B] (1998) Khan, F. I., & Abbasi, S. A., "Risk assessment in chemical process industries: Advance techniques", New Delhi: Discovery Publishing House. (XC376).

- [11] J] Khan, F. I., and Abbasi S. A., (2000).. “Analytical simulation and PROFAT II: A new methodology and a computer automated tool for fault tree analysis in chemical process industries”’. *Journal of Hazardous Materials*, 75, 1–27. (2000)
- [12] J] Khan, F. I., and Haddara, M. R., (2003), “Risk-based maintenance (RBM): A quantitative approach for maintenance/inspection scheduling and planning” *Journal of Loss Prevention in the Process Industries*, 16, 516–573.
- [13] J] Khan, F. I., and Haddara, M. R. (2004), “Risk-based maintenance of ethylene oxide process plant”, *Journal of Hazardous Materials*, A108, 147–159.
- [14] B] Kletz T. A., (1994), “What went wrong. Houston”, Gulf Publication House.
- [15] J] Kumar, U., “Maintenance strategies for mechanized and automated mining systems; a reliability and risk analysis based approach”. *Journal of Mines, Metals and Fuels, Annual Review*, 343–347. (1998).
- [16] C ] Misewicz, D., Smith, A. C., Nessim, M., and Playdon, D (2002), “Risk based integrity project ranking”, *Proceedings of IPC'02, IPC2002-27214*.
- [17] BC] Montgomery L. R., and Serratela C., (2002), “Risk-based maintenance: A new vision for asset integrity management” *Selected topics on aging management, reliability, safety and license renewal, ASME, PVP, (Vol. 444)*. (2002).
- [18] J ] Murty, A.S.R. and Naikan V.N.A. (1996) “Condition monitoring strategy-a risk based interval selection”, *International journal of Production Research*, vol 1, pp. 285-96
- [19] J ]Shore ,H. (1996), “Optimum schedule for preventive maintenance, a general solution for a partially specified time to failure distribution” *Production and Operation Management*, vol 5, no 2, pp 148–62.
- [20] J] Vaurio J. K., (1995), “Optimization of test and maintenance intervals based on risk and cost”, *Reliability Engineering and System*, 49, 23–36.
- [21] Krishnasamy L, Khan F and Haddara M. “Development of Risk based maintenance strategy for a power generating plant” in the *journal of Loss prevention in the process industries*, vol 18, pp 69–81, 2005.

# Instructions for Authors

## Essentials for Publishing in this Journal

- 1 Submitted articles should not have been previously published or be currently under consideration for publication elsewhere.
- 2 Conference papers may only be submitted if the paper has been completely re-written (taken to mean more than 50%) and the author has cleared any necessary permission with the copyright owner if it has been previously copyrighted.
- 3 All our articles are refereed through a double-blind process.
- 4 All authors must declare they have read and agreed to the content of the submitted article and must sign a declaration correspond to the originality of the article.

## Submission Process

All articles for this journal must be submitted using our online submissions system. <http://enrichedpub.com/> . Please use the Submit Your Article link in the Author Service area.

---

## Manuscript Guidelines

The instructions to authors about the article preparation for publication in the Manuscripts are submitted online, through the e-Ur (Electronic editing) system, developed by **Enriched Publications Pvt. Ltd.** The article should contain the abstract with keywords, introduction, body, conclusion, references and the summary in English language (without heading and subheading enumeration). The article length should not exceed 16 pages of A4 paper format.

### Title

The title should be informative. It is in both Journal's and author's best interest to use terms suitable. For indexing and word search. If there are no such terms in the title, the author is strongly advised to add a subtitle. The title should be given in English as well. The titles precede the abstract and the summary in an appropriate language.

### Letterhead Title

The letterhead title is given at a top of each page for easier identification of article copies in an Electronic form in particular. It contains the author's surname and first name initial .article title, journal title and collation (year, volume, and issue, first and last page). The journal and article titles can be given in a shortened form.

### Author's Name

Full name(s) of author(s) should be used. It is advisable to give the middle initial. Names are given in their original form.

### Contact Details

The postal address or the e-mail address of the author (usually of the first one if there are more Authors) is given in the footnote at the bottom of the first page.

### Type of Articles

Classification of articles is a duty of the editorial staff and is of special importance. Referees and the members of the editorial staff, or section editors, can propose a category, but the editor-in-chief has the sole responsibility for their classification. Journal articles are classified as follows:

#### Scientific articles:

1. Original scientific paper (giving the previously unpublished results of the author's own research based on management methods).
2. Survey paper (giving an original, detailed and critical view of a research problem or an area to which the author has made a contribution visible through his self-citation);
3. Short or preliminary communication (original management paper of full format but of a smaller extent or of a preliminary character);
4. Scientific critique or forum (discussion on a particular scientific topic, based exclusively on management argumentation) and commentaries. Exceptionally, in particular areas, a scientific paper in the Journal can be in a form of a monograph or a critical edition of scientific data (historical, archival, lexicographic, bibliographic, data survey, etc.) which were unknown or hardly accessible for scientific research.



**Professional articles:**

1. Professional paper (contribution offering experience useful for improvement of professional practice but not necessarily based on scientific methods);
2. Informative contribution (editorial, commentary, etc.);
3. Review (of a book, software, case study, scientific event, etc.)

**Language**

The article should be in English. The grammar and style of the article should be of good quality. The systematized text should be without abbreviations (except standard ones). All measurements must be in SI units. The sequence of formulae is denoted in Arabic numerals in parentheses on the right-hand side.

**Abstract and Summary**

An abstract is a concise informative presentation of the article content for fast and accurate Evaluation of its relevance. It is both in the Editorial Office's and the author's best interest for an abstract to contain terms often used for indexing and article search. The abstract describes the purpose of the study and the methods, outlines the findings and state the conclusions. A 100- to 250-Word abstract should be placed between the title and the keywords with the body text to follow. Besides an abstract are advised to have a summary in English, at the end of the article, after the Reference list. The summary should be structured and long up to 1/10 of the article length (it is more extensive than the abstract).

**Keywords**

Keywords are terms or phrases showing adequately the article content for indexing and search purposes. They should be allocated heaving in mind widely accepted international sources (index, dictionary or thesaurus), such as the Web of Science keyword list for science in general. The higher their usage frequency is the better. Up to 10 keywords immediately follow the abstract and the summary, in respective languages.

**Acknowledgements**

The name and the number of the project or programmed within which the article was realized is given in a separate note at the bottom of the first page together with the name of the institution which financially supported the project or programmed.

**Tables and Illustrations**

All the captions should be in the original language as well as in English, together with the texts in illustrations if possible. Tables are typed in the same style as the text and are denoted by numerals at the top. Photographs and drawings, placed appropriately in the text, should be clear, precise and suitable for reproduction. Drawings should be created in Word or Corel.

**Citation in the Text**

Citation in the text must be uniform. When citing references in the text, use the reference number set in square brackets from the Reference list at the end of the article.

**Footnotes**

Footnotes are given at the bottom of the page with the text they refer to. They can contain less relevant details, additional explanations or used sources (e.g. scientific material, manuals). They cannot replace the cited literature.

The article should be accompanied with a cover letter with the information about the author(s): surname, middle initial, first name, and citizen personal number, rank, title, e-mail address, and affiliation address, home address including municipality, phone number in the office and at home (or a mobile phone number). The cover letter should state the type of the article and tell which illustrations are original and which are not.

**Address of the Editorial Office:****Enriched Publications Pvt. Ltd.**

S-9, IInd FLOOR, MLU POCKET,  
MANISH ABHINAV PLAZA-II, ABOVE FEDERAL BANK,  
PLOT NO-5, SECTOR -5, DWARKA, NEW DELHI, INDIA-110075,  
PHONE: - + (91)-(11)-45525005

Notes:

[illegible]